



Open
Access

Development and Test Performance of Heterogeneous Catalysts on Steam Reforming of Bioethanol for Renewable Hydrogen Synthesis: A Review

A. N. Isah^{1,2}, E. J. Eterigho², M. A. Olutoye², M. U. Garba², I. P. Okokpujie^{3,*}

¹ Department of Chemical Engineering Technology, School of Engineering Technology, Federal Polytechnic Nasarawa, Nasarawa State, Nigeria

² Department of Chemical Engineering, School of Infrastructure, Process Engineering and Technology, Federal University of Technology, Minna, Niger State, Nigeria

³ Department of Mechanical Engineering, Covenant University, Ota, Ogun State, Nigeria

ARTICLE INFO

Article history:

Received 27 March 2020

Received in revised form 24 April 2020

Accepted 28 April 2020

Available online 5 July 2020

ABSTRACT

The demand for sustainable energy supply due to the significant population growth has led to the search for more energy generation sources to assist the depleting fossil fuel energy. This clean energy source will help in eliminating the environmental challenges posed by conventional fossil fuel. However, this research focuses on high efficient energy resources area to obtain sufficient energy from the hydrogen fuel cell. The hydrogen fuel cell is considered as an option because it releases water as a by-product during combustion and possesses high energy density per mass of 120.7kJ/kg compared to other fuels, with three times more energy content than gasoline. However, hydrogen production is predominantly from fossil-based feedstock via steam reforming over nickel-based catalysts. Because of the carbon footprint and fossil resource depletion, attention is being shifted to non-fossil based feedstock to reduce greenhouse gas emission and enhance energy efficiency. During steam reforming of hydrocarbon, catalysts help to activate and rupture the C-C and C-H bonds. This paper discusses the recent development of solid catalysts, the preparation method, catalytic activity, selectivity and reusability, level of conversion of the reactants, yield, and purity of hydrogen. The structural modifications of the catalysts are also discussed based on actual metal particle size, the oxidation state of the based metal, spatial distribution of the metal on the reducible oxide support, and microstructure of the catalyst. This study concluded that a better catalyst system would improve the efficiency of hydrogen yield due to the displacement of the thermodynamic equilibrium of the product.

Keywords:

Fossil fuels; hydrogen; fuel cell; steam reforming; catalyst; deactivation

Copyright © 2020 PENERBIT AKADEMIABARU - All rights reserved

* Corresponding author.

E-mail address: imhade.okokpujie@covenantuniversity.edu.ng; isnab2006@yahoo.com

<https://doi.org/10.37934/arfmts.73.1.69108>

1. Introduction

High energy demand, climate change, and global warming are the touching challenges facing the world at the moment [1-2]. Therefore, the need for sustainable energy usage as an alternative to fossil fuels for industrial and domestic activities has become evident and urgent. The non-fossil fuel to be considered as a substitute to the conventional fuel must be clean, replenish-able, and sustainable energy supply source [3-4]. Sustainable energy intakes such as solar, wind, geothermal, and biomass have gained attention as carbon neutral about environmental impacts compared with fossil fuels [5]. Also, the rapid depletion of conventional fuel has necessitated the introduction of bio-hydrogen into the energy mix, especially for fuel cell application. Fuel cells could be driven by chemical via electrodes or metabolism of organic wastes (i.e. wastewater and plant extract) using microorganism to generate electricity [6]. According to Yahya *et al.*, [7] Plant microbial fuel cell is one of the emerging approaches to generate green electricity via metabolic of plant rhizodeposits using bacteria. However, electricity generation by this approach is still at the laboratory scale and before it can be commercialized, there is a need to increase proton transport. Also, the reduction of oxygen transport to decline the internal resistance of microbial fuel cell via the application of a mixed culture of aerobic bacteria. It is due to this downturn that makes chemical fuel cell readily available and widely in use. Fuel cell transforms the inherent chemical energy in hydrogen fuel into electric power via electrochemical reactions. Hydrogen has been confirmed as a potential energy carrier for development of sustainable energy systems. It serves as a feedstock in a fuel cell to generate electricity at high efficiencies (85%) with low environmental impact, as water is the only product of the reaction [8][9]. Hydrogen is a candidate for clean energy source when combined with polymer electrolyte membrane fuel cell (PEMFC) technology, and has the potential to play a very vital role in power generation system in the future for both mobile and stationary applications [10-11]. Hydrogen has high efficiency of conversion via reformer to usable power, low generation of pollutants, and high energy density. It has a high energy yield (122kJ/g), which is 2.75 times greater than hydrocarbon fuels [12].

The possibility of the future hydrogen (H₂) economy lies in the development of efficient, large-scale and sustainable H₂ production systems because 95% of the hydrogen produced as of today comes from non-renewable resources [13]. Hydrogen production is classified into physiochemical, electrochemical, and biological processes. The existing physicochemical methods (such as steam reforming of hydrocarbons and coal gasification) are neither sustainable nor environmental benign because conventional fuels are used as substrate. Presently, hydrogen is being produced globally with fossil fuel-based technologies like natural gas steam reforming (49% of worldwide H₂ supply), 29% from light oil (naphtha), 18% from coal gasification, 3.9% by water electrolysis, and 0.1% via other sources [14]. In an attempt to amend the effect of carbon (IV) oxide emission via the usage of harmful carbon fuels, a combination of renewable energy and biofuels could be harnessed to achieve the target. Ulhiza *et al.*, [15] carried a review on the process of using dark fermentative bacteria in the production of biohydrogen through waste from the starch. The authors concluded that among the biological processes of hydrogen production, dark fermentation of organic waste (i.e. starch-containing waste) using fermentative bacteria shows the simpler mechanism in terms of preparation, and gives better yield when compared to photo-biological processes [15]. However, the bottleneck in its commercialization is lack of efficient pre-treatment technique of the organic waste on a large scale. The cost-effective and more straightforward mechanism of reducing the greenhouse gases emission is through the catalytic conversion of biofuels through reforming. Biofuel produced from biomass (non-food agricultural resources), which is relatively cheap and readily available feedstock, helps in balancing the carbon cycle through the photosynthesis process. Dilute bio-ethanol is a typical

feed for ethanol steam reforming, which is produced by serial of methods of pretreatment of lignocellulosic materials, hydrolysis, and fermentation [16-17]. Among the renewable resources for hydrogen production, ethanol has gained attention because of its relatively high hydrogen content, easily generated in large quantity from abundant biomass resources, free from sulphur-containing compounds, readily available, eco-friendly, as well as better safety in terms of storage and handling [18-19].

The steam reforming (SR), partial oxidation (POX), and auto-thermal reforming (AR) are effective methods for harnessing hydrogen from bio-ethanol. Among the reforming methods, steam reforming is one of the most widely studied routes of producing hydrogen because of its high efficiency, low operational, production costs, and it guarantees high hydrogen yield. However, steam reforming of ethanol (SRE) generates a high hydrogen/carbon (II) oxide ratio. Still, it has the disadvantage of being high endothermic and catalyst inactiveness due to carbon formation and sintering of active metals. Meanwhile, partial oxidation reduces the problem of energy consumption since it is exothermic; its disadvantage is a low hydrogen/carbon (II) oxide ratio formation [20]. However, in auto-thermal reforming, the oxygen separation unit is expensive to run, and the catalyst is prone to deactivation easily as a result of oxygen inclusion, which favours sintering, without negating the tendency for coke formation [21]. As such, steam reforming of ethanol possesses the highest potential to be commercialized soon. However, the success story of steam reforming lies in the stability and activeness of catalysts employed. The development of active and efficient catalysts is essential for the possibility of large scale hydrogen production through ethanol steam reforming. So many catalysts have been investigated, majorly based on noble metals such as Ir, Rh, Pt, Ru, and Pd and non-noble metals such as Ni, Co, and Cu [22-23]. Noble metals exhibit high catalytic activity and stability when used in steam reforming reactions. Still, despite their excellent catalytic performance, it is not a wise choice because of economic reasons and their scarcity [24]. Nickel, copper, and cobalt are mostly used as catalysts in the ethanol steam reforming process because of their excellent catalytic activity and low cost [25]. Nickel is prioritized due to its high activity for C-C bond and O-H bond breaking and its influence on the formation of molecular hydrogen. However, coke formation and sintering of metal particles deactivate the industrial nickel catalysts, due to the endothermic nature of steam reforming and the high tendency of catalyst poison from either by-product influence or due to impurities associated with the feed. These defects can be reduced by modifying the catalyst with support, due to their chemical effect, apart from their interaction with the active phase.

The interactions between base metal and support give rise to surface effects, which could be geometric or electronic influence. The results have an essential stake in the catalytic activity since most reactions are dependent on the surface atoms. Also, supports with sufficient surface area and small pores usually exhibit additional mass transfer limitation issues of the reactants [26-27]. At higher temperatures, some supported catalysts are still prone to coke deposition and base metal sintering problem. Similarly, transport of small molecules is governed by gaseous diffusion, which leads to low hydrogen selectivity, while other gases will permeate simultaneously [28]. The alleviate the setback and advance the catalytic efficiency of the supported catalysts, and there is a need to improve properties of the support, use of a better formulation for active metal loading, and method of enzymes preparation [29]. Several types of research have been conducted on the possibility of improving the catalytic performance of either single-metal based catalysts or multiple component catalysts. With the importance of catalysts in the reaction mechanism of steam reforming, this article reviews current researches on the catalyst preparation and methods. Also, consider experimented catalyst compositions, influence of active metals (noble and non-noble metals) on catalytic activity, catalytic support materials, catalyst modification techniques. Factors that determine catalytic performance, metal-catalytic support interaction, catalyst decay, the highlight of different catalyst

decay mechanisms, and kinetics. And deactivation prevention during steam reforming of hydrocarbon resources for hydrogen production as the ultimate goal in catalysis. Research is to develop novel active and selective catalysts for a heterogeneous catalyst for targeted test reaction. This article will serve a useful purpose in terms of the selection of preferred activities and support material for catalyst preparation and method, usage conditions, and catalyst decay preventive mechanisms.

2. Hydrogen as An Energy Carrier

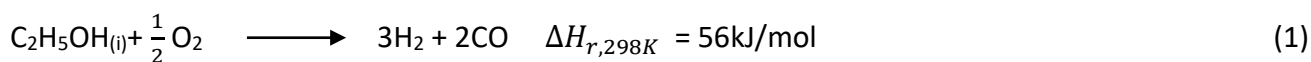
Hydrogen is among the most promising fuels as a potential energy source, being replenish-able and eco-friendly. It evolves a tremendous amount of energy per unit weight in combustion and is easily convertible to electricity by fuel cells [30]. Hydrogen is used for energy services, especially in the transport sector, and for power generation using hydrogen gas turbines [31].

2.1 Hydrogen Production Through Reforming of Ethanol

Hydrogen is produced through the reforming of light hydrocarbons such as natural gas, methanol, ethanol, and glycerol. Ethanol is preferable as a substrate for reforming due to its relatively high hydrogen content, oxygenated nature, readily available, eco-friendly, as well as better safety in terms of storage and handling. Also, ethanol can be produced from readily available biomass. The conventional reforming methods of producing hydrogen from ethanol are ethanol steam reforming, partial oxidation reforming of ethanol, and auto-thermal reforming of ethanol. Ethanol steam reforming is simply under thermodynamics indices and tends high yield of hydrogen.

2.1.1 Partial oxidation reforming of ethanol

It is the incomplete combustion of ethanol with a limited supply of oxygen gas at a temperature range of 200-300°C, with the inclusion of catalysts to yield carbon (II) oxide and hydrogen. Oxygen is very active in partially oxidizing ethanol for hydrogen production, as depicted in Eq. (1), which requires less energy input for reaction takes off. It was reported that 51% ethanol conversion and 97% H₂ selectivity had been successively obtained through this process at a temperature as low as 370°C over Pt/ZrO₂ [32].



2.1.2 Auto-thermal reforming of ethanol

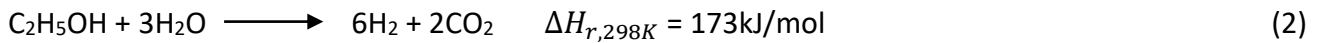
In auto-thermal reforming of ethanol, ethanol is mixed with steam and pure oxygen and air at the top of the reactor. In the same combustion chamber, the heat generated from partial oxidation reactions is utilized for endothermic steam reforming reactions. The steam reforming and shift conversion reactions occur as the reactant gases pass through the fixed bed (loaded with changing catalyst) to form a relative gas mixture of hydrogen, carbon (II) oxide, and carbon(IV) oxide [33].

2.1.3 Ethanol steam reforming (ESR)

The prevalent method of producing abundant hydrogen gas is the steam reforming of ethanol, which is the endothermic conversion of ethanol (C₂H₅OH) and steam at 200 to 800 °C. Furthermore,

the pressures of 1 to 3 bar, in the presence of a metal-based catalyst (nickel), to produce hydrogen and carbon (II) oxide (CO). Subsequently, CO produced (about 12%) is converted to carbon (IV) oxide (CO₂) and hydrogen (H₂) via the water-gas shift reaction (WGS) [34-35].

Ethanol steam reforming reaction with adequate steam supply:



Ethanol steam reforming reaction with inadequate steam supply:

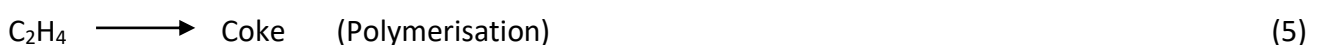


Steam reforming of ethanol involves the cleavage of C-C bond, the reaction mechanism for steam reforming of ethanol is more complicated, and many side reactions may occur [30]. Steam reforming of light alcohols like ethanol and methanol is a priority area to realize hydrogen economy in the future. Steam reforming is operated at low pressure because it involves volume expansion. In contrast, the exothermic shift reaction is conducted at low temperature, without considerable effect on pressure changes. WGS is a reversible reaction that, at lower temperatures, shifts the equilibrium to the right favouring the formation of the hydrogen and carbon (IV) oxide.

Moreover, at higher temperatures, the reaction kinetics is quicker and reaction toward to lower conversion of carbon (II) oxide [35]. Change in molar totals does not affect WGS reaction, and as such, the effect of pressure on the response is minimal. However, hydrogen production at equilibrium is favoured at low temperature and high moisture content, via an exothermic reaction. Liguras *et al.*, [36] reported that at higher temperatures (873-1073K), conversion of ethanol as well as selectivity of carbon (II) oxide, carbon (IV) oxide, and hydrogen, gets increased.

2.2 The possible Reaction Pathways Associated with Steam Reforming of Ethanol

During the reforming of ethanol, undesired products are formed because of simultaneous reactions by breaking of the C-O bonds of the oxygenated organic, developing alcohols or organic acids. The reaction mechanisms associated with the ethanol steam reforming process are complicated, based on the catalyst preparation, forms, and shape. Based on the operating conditions and the choice of catalyst, ethanol reforming reactions are usually associated with undesired product formation (such as acetaldehyde, methane, ethylene, carbon monoxide). Due to the several reaction pathways occurring, as shown in Figure 1 [37]. Ethanol conversion could be possible in the form of dehydrogenation to acetaldehyde, dehydration to ethylene, or decomposition to methane and carbon dioxide. Boudouard reaction, ethylene polymerization, and methane decomposition are responsible for the coke formation on the catalyst surface (as presented in Eqs. (5)-(7), which is detrimental to the efficiency of ethanol steam reformer [38-39].



In this regard, for proper conversion of the bio-resources (ethanol) to obtain the desired product at considerable energy and low carbon footprint, there is a need for the development of durable, high activity and selective catalysts.

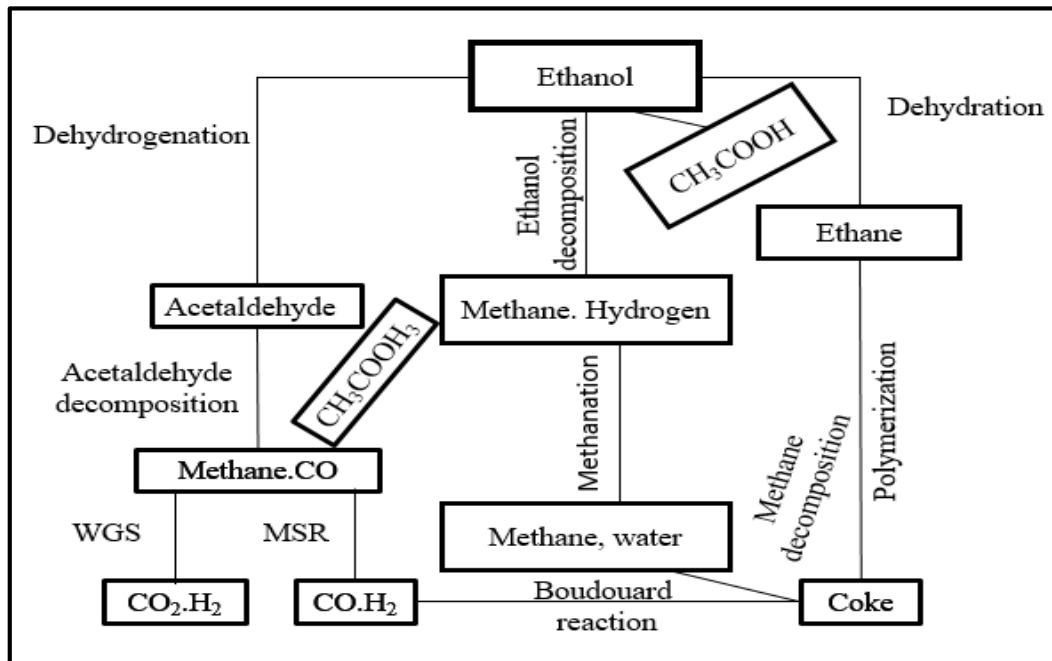


Fig. 1. Reaction mechanism tendency for ethanol steam reforming

2.3 Heterogeneous Catalyst

A heterogeneous catalyst consists of constituents like support, promoter, and active catalytic ingredients of metal or metal oxides/solid acids. Pure metals could be applied as heterogeneous catalysts or sprinkled as small grains on the surface of supporting material. As catalysis is a surface reaction, it is essential to have adequate knowledge of local surface chemistry of the catalyst, being a basis of its catalytic activity. Heterogeneous catalysis is based on chemisorption phenomena because the reaction takes place at temperatures above the critical temperatures of the reactants involved since physical adsorption cannot occur under these conditions. Heterogeneous catalysis demands catalyst supports with high hydrothermal, mechanical stability, and high specific area because the active component requires high accessibility since diffusion has an essential function in the reaction rate. The catalytic performance depends on intrinsic (i.e., thermodynamics and kinetics) and extrinsic (hydrodynamics and transport phenomena) processes [40-42].

2.3.1 Based metal for heterogeneous catalyst

Out of several enzymes tested so far for ethanol reforming, transition metals mainly, nickel and cobalt (Ni and Co) perform excellently in the cleavage of C-C, C-H, and C-O. In contrast, noble metals (Pt, Pd, Rh) have been widely used for water-gas shift reaction because of their high activity and low tendency to coke formation [43]. Nickel offers excellent corrosion resistance, toughness, strength at high and low temperatures, and a range of distinctive magnetic and electronic properties. Nickel is comparable to Pd and Pt in terms of electronic properties; as such, its usage can serve as a substitute in reaction, which the duo can help. Ni can be partially oxidized when used on the surface of the

catalyst due to its relatively low reduction potential, and in turn, enhance its catalytic performance [44].

Similarly, it has been reported that bimetallic catalysts lead to high catalytic effectiveness in the ethanol steam reforming reaction. However, the doping with second metal plays a vital role in improving reducibility, discouraging sintering, and hindering deactivation due to coke formation. Among the studied metal-metal used are Ni-Co, Rh-Co, Cu-Ni, Pt-Ni, Pt-Co, and Rh-Pt [45] [46]. Because of the affordability and easy accessibility of nickel, it is widely considered as the base metal for catalyst synthesis to facilitate ethanol steam reforming process [46]. Thyssen *et al.*, [47] reported that Ni catalysts favour the C-C cleavage of the alcohols, leading to CH₄, CO, and H₂ development. Still, these catalysts are also known to maintenance the deposition of carbon, which may damage the performance of the enzyme.

2.3.2 Support/promoter for heterogeneous catalyst

Irrespective of active metal or promoter selected for the supported catalysts, support with a high surface area is a vital factor that can enhance the catalytic performance. The type of backing used on active metal also influences the catalytic activity of the modified catalyst in terms of surface area, porous structure, mechanical strength, and chemical interaction between the metal and support. Based on surface chemical properties of the support, it can be classified in four major groups: essential supports (MgO, CaO, BaO), acidic supports (γ -Al₂O₃, SiO₂, Al₂O₃/SiO₂, zeolites), neutral supports (MgAl₂O₄, MgCr₂O₄, ZrCrO₄, ZnAl₂O₄), and amphoteric supports (α -Al₂O₃, TiO₂, CeO₂, ZrO₂). The widely reported supports for steam reforming are γ -Al₂O₃, MgO, MgAl₂O₄, SiO₂, ZrO₂, and TiO₂. These supports possess good porosity, which paves the way for better contact between reactants and catalyst. Using porous support with an adequate pore texture eliminates diffusional limitations that often encountered during fluid-solid catalyst interaction [48-50]. When active metal particles are dispersed on oxide-grounded supports, their catalytic performances are seriously improved compared to those of pure metal particles. Using micro-sized metal particles, it grows into larger crystallites upon high-temperature annealing, resulting in a fabulous significant loss of their catalytic activities [51]. The level of dispersion of active metal on support and the resistance of as-synthesised catalyst to sintering is dependent on the quality of the support. It equally alters the reactivity and coke resistance of the base metal particles and could participate in the reaction at times. Abad-Elwahad *et al.*, [52] and Eterigho *et al.*, [53] confirm that during the addition of catalyst with oxide support material (i.e. alumina), the physiochemical attributes like thermal resistance and oxidation state of solid catalysts would be re-structured by the amalgamation process.

2.3.2.1 Influence of support on the heterogeneous catalyst performance

Support materials influence the effect on the structure and physicochemical characteristics of the supported catalyst. Hamzah and Yarmo [54] studied the effect of bentonite, titanium oxide (TiO₂), aluminium (III) oxide (Al₂O₃) and silicon (IV) oxide (SiO₂) (as support) for the catalyst for hydrogenolysis of glycerol. It was found that the bentonite supported Ru-bentonite supported catalyst has an outstanding glycerol conversion of 62.8% compared to other used supports. This is attributed to the average particle size of Ru/bentonite, being the smallest among the catalyst studied, as confirmed by TEM, and the excellent dispersion of Ru particle on the bentonite support compared to other supports, as approved by FESEM. Also, bentonite is essential to support, while TiO₂, Al₂O₃, and SiO₂ are acidic support. This is the basis for its high activity that enables glycerol conversion reached 62.8% and selectivity to 1,2-propanediol (80.1%) compared to other catalysts which are

supported with TiO_2 , Al_2O_3 , and SiO_2 respectively. Ali *et al.*, [55] investigated the influence of support on the catalytic performance of the nano-Au catalysts for complete propane oxidation. The reactions were carried out in a reactor with PID micro-activity reference temperature ranges from 30 to 450°C at $24000\text{h}^{-1}\text{GHSV}$ using 0.5g of the catalyst. CeO_2 , ZrO_2 , and the $\text{CeO}_2\text{-ZrO}_2$ are the supports used to synthesize $\text{Au}_{\text{HAuCl}_4}\text{-Ce}$, $\text{Au}_{\text{HAuCl}_4}\text{-Zr}$, and $\text{Au}_{\text{HAuCl}_4}\text{-Ce-Zr}$, respectively. At 400°C of catalytic tests of the catalysts, Au-CeO₂ supported catalyst oxidized the propane by 40%; over ZrO₂-Au supported catalyst, the propane was converted by less than 5%, and Au helped with the CeO₂-ZrO₂ nearly oxidized the propane by 10%. The excellent catalytic performance of $\text{Au}_{\text{HAuCl}_4}\text{-Ce}$ is associated with its surface area, crystallinity, phase structure, and redox attribute of the support used.

Zhang *et al.*, [56] researched the effect of selected supports (TiO_2 , Al_2O_3 , and CeO_2) on Ag-based catalysts synthesised by the impregnation approach and used for the catalytic oxidation of formaldehyde (HCHO) at low temperature. Ag/TiO₂ catalyst proved excellent catalytic activity for 100% conversion of 110ppm HCHO at near 95°C . The characterization results revealed that Ag/TiO₂ catalyst possessed the smallest Ag particle size and highest Ag dispersion.

Ogo *et al.*, [57] researched the influence of various hydroxyapatite supports for ethanol steam reforming. The synthesized hydroxyapatite-supported Co catalysts are $\text{Co/Ca}_{10}(\text{PO}_4)_6(\text{OH})_2$, $\text{Co/Sr}_{10}(\text{PO}_4)_6(\text{OH})_2$, $\text{Co/Ca}_{10}(\text{VO}_4)_6(\text{OH})_2$ and $\text{Co/Sr}_{10}(\text{VO}_4)_6(\text{OH})_2$. It was discovered that $\text{Co/Sr}_{10}(\text{PO}_4)_6(\text{OH})_2$ Catalyst yielded the highest conversion and hydrogen yield compared to other prepared incentives. The high catalytic activity of $\text{Co/Sr}_{10}(\text{PO}_4)_6(\text{OH})_2$ the catalyst for steam reforming is mainly because of its essential nature compared with other synthetic enzymes. In terms of coke depression ability, $\text{Co/Sr}_{10}(\text{PO}_4)_6(\text{OH})_2$ the catalyst was tested for product selectivities via ethanol steam reforming and showed lower ethylene selectivity, being the major coke precursor. Subsequently, the coke formation on $\text{Co/Sr}_{10}(\text{PO}_4)_6(\text{OH})_2$ the catalyst was quantified to be $12\text{mg g}^{-1}\text{cat}^{-1}$ after 185min of reaction, which is far less than the reported carbon deposition on conventional $\text{Co}/\alpha\text{-Al}_2\text{O}_3$ catalyst ($420\text{ mg g}^{-1}\text{cat}^{-1}$). The catalyst's ability to suppress coke formation is due to its electronic state, as confirmed using X-ray absorption fine structure (XAFS). As such, $\text{Co/Sr}_{10}(\text{PO}_4)_6(\text{OH})_2$ catalyst is the right candidate for coke formation suppression.

Olivares *et al.*, [58] studied the influence of the addition of ether Na or K on support in terms of ethylene formation (a coke formation precursor) by changes in the surface acidity of the catalyst. The prevention of carbon deposition is possible through a designated Ni particle size; Ni particles less than 10nm (critical size) with high dispersion on support could reduce the carbon deposition or the pressure increase in the catalyst horizon (bed). Bergamaschi and Carvallo [59] investigated the catalytic performance of zirconia and alumina supported Cu/Ni catalyst microspheres synthesized by hydrolysis approach for hydrogen production via ethanol steam reforming. The Cu/Ni/ZrO₂ and Cu/Ni/Al₂O₃ were prepared with different compositions and tested for catalytic performances. It was discovered that Cu/Ni supported on zirconia give higher selectivity in favour of hydrogen. Several results gathered over zirconia and alumina supported catalysts with an equal Cu/Ni content show that proper interaction of Cu/ Ni and helps plays a vital stake in the reaction. Basic oxide like zirconia has been reported to serve as an inhibitor to ethylene formation. In summary, the influence of support on the performance of a synthesized catalyst depends on the average particle size of the support, its fundamental nature, and its level of interaction and dispersion on the base metal.

2.3.2.2 The Influence of promoter on the heterogeneous catalyst performance

Abbasi *et al.*, [60] investigated the influence of lanthanum, being a promoter on Fe-Co/SiO₂ catalyst for Fischer-Tropsch synthesis. Fe-Co/SiO₂ and La- Fe-Co/SiO₂ catalysts were prepared by wet impregnation approach, characterized and tested in a quartz reactor for their catalytic activities. It

was discovered that lanthanum loading partially decreases the reduction temperature of the as-prepared catalysts. The minimization of reduction temperature lowers the partial oxidation, and in turn, catalyst sintering. Also, the inclusion of lanthanum gave better performance property to the catalyst in terms of C_1 - C_4 and C_5^+ production by minimizing the CO_2 selectivity and operating temperature of the process.

Zamani *et al.*, [61] studied the effect of calcium (as a promoter) on nanostructured iron catalyst morphology, activity, and product selectivity in Fischer-Tropsch synthesis. Nanostructured iron catalysts were prepared by a macro-emulsion method. The test reactions were carried out in a fixed bed stainless steel reactor. The composition of the resultant nanosized iron catalysts concerning the atomic ratio was 100Fe/4Cu, 100Fe/4Cu/2Ca, and 100Fe/4Cu/4Ca, respectively. It was discovered that the inclusion of Ca promoter increases the iron derived catalyst activity, and the 100Fe/4Cu/2Ca showed the best performance between the prepared catalysts. Dan *et al.*, [62] investigated the influence of Au/Ag/Cu promoted on Ni-alumina supported catalyst for steam reforming of ethanol. The catalysts synthesized were Ni-Ag/Al, Ni-Au/Al, and Ni-Cu/Al concerning nickel content of 6wt%, 6.8wt%, and 6.1wt%, respectively, while Ni/Al catalyst serves as reference catalyst. From the TPR profile, it showed that the inclusion of the noble metals (Ag, Au) to Ni/Al has the effect of bringing down the principal peak reduction from 735 °C for Ni/Al to 534°C for Ni-Ag/Al and 557°C for Ni-Au/Al. The adding of copper to Ni/Al has a comparable effect by reducing the temperature of the central reduction peak to 672°C from 735°C.

In summary, the addition of the three metals (as promoters) to Ni/Al₂O₃ decreases the ability of NiO_x mingling with the support increasing, thus the reducibility of catalyst precursor. Souza *et al.*, [63] worked on the structural modification and performance of Ni-Al hydrotalcite-type catalysts, promoted with Mg, Zn, Mo, and Co for steam reforming of ethanol. XRD results showed that partly replacement of Ni by Zn, Mo, or Co results in a decrease in the crystallinity, which leads to smaller crystallites formation. The H₂-TPR profiles revealed that the existence of broad reduction peaks at temperatures between 600 and 800°C for all the samples indicate a near impossible reduction of NiO to Ni⁰. Using the test reaction for the catalytic test showed that the dehydration and dehydrogenation of ethanol occur at lower temperatures, while higher temperatures induced the formation of synthesis gas.

2.3.2.3 The influence of the precursor on the heterogeneous catalyst performance

The selection of precursor lies on parameters like the support attributes and the preconditions for the targeted metal particle size. Regarding the effect of the Au precursors on the activity, three different Au precursors, H₂AuCl₄·3H₂O, AuBr₃, and AuI, were used to develop catalysts with CeO₂ support. At 520°C, Au_{H₂AuCl₄}-Ce catalyst possessed the highest catalytic performance (nearly 100% conversion), Au_{AuI}-Ce converted the propane by 60% while Au_{AuBr}-Ce achieved 50% conversion of propane. Au dispersion of catalyst synthesized from H₂AuCl₄·3H₂O on the support could be attributed to the high solubility constant of H₂AuCl₄·3H₂O (as a precursor) [64]. Dey *et al.*, [65] studied the influence of the choice of precursors in preparing CuMnO_x catalysts for enhancing CO oxidation. CuMnO_x catalyst was prepared by the co-precipitation approach with various types of precursors. The precursors precipitated by KMnO₄ solution were {Mn(AC)₂+ Cu(NO₃)₂}, {Mn(AC)₂+ Cu(AC)₂}, {Mn(NO₃)₂+ Cu(NO₃)₂} and {Mn(NO₃)₂+ Cu(AC)₂} respectively. After catalyst tests, it was discovered that the catalyst synthesised by {Mn(AC)₂+ Cu(NO₃)₂} as a precursor showed the best catalytic performance towards CO, because of their high oxygen mobility.

Alube *et al.*, [66] investigated the influence of cerium precursors in the preparation of Ce-MCM-41 and the capacity for liquid-phase oxidation of benzyl alcohol. Ce-MCM-Cl and Ce-MCM-NO₃ were

respectively synthesized from $\text{CeCl}_3 \cdot 7\text{H}_2\text{O}$ and $\text{Ce}(\text{NO}_3)_3 \cdot 6\text{H}_2\text{O}$ as precursors. The catalytic performance of the catalysts was verified in the liquid-phase oxidation of benzyl alcohol (BZOH) with tert-butyl hydroperoxide (TBHP) to produce benzaldehyde (BZD). It was found out that Ce-MCM-Cl obtained better BZOH transformations and benzaldehyde yields, while Ce-MCM- NO_3 showed improved BZD selectivity. Jedrzejewski and Lendzion-Bielum [67] investigated the effect of oxides of calcium, aluminium, and lithium (as precursors) on iron catalysts synthesized by a fusion method. It was discovered that catalyst precursors had a magnetite structure—lithium oxide yielding the solid solution in magnetite facilitated phase reduction. Catalysts promoted with lithium oxide showed high activity, with an increased degree of modification. Structural promoters like calcium and aluminium oxides, guarding iron against sintering, were released during the magnetite phase reduction. Furthermore, formed a three-dimensional (3-D) structure; it implies they built bridges between iron crystallites.

2.3.2.4 The Influence of the preparation method on the heterogeneous catalyst performance

Preparation method determines the structural attributes and catalytic activity of the catalyst. The redox properties and reactivity of as-synthesised catalysts depend on the modifications of the surface area, particle size, dispersion of the active component, and strength of the interaction between the active metal and the support. Zhang *et al.*, [68] investigated the catalytic performance of Ag- Fe_2O_3 catalysts prepared by wet impregnation, hydrothermal method, and conventional impregnation method, respectively. The synthesized catalysts were tested for CO oxidation in a continuous flow fixed bed reactor system. The synthesized catalysts were respectively named Ag-MIL, Ag- Fe_2O_3 , and Ag-PB, based on the constituent based metal, support, and method of preparation. It was discovered that Ag-MIL prepared by impregnation method has the best structure and catalytic performance among the catalysts, due to its Ag^0 species and large specific surface area.

Jhung *et al.*, [69] investigated the effect of preparation methods on the catalytic activity and metal diffusion of Pt/C and Pd/C catalysts for hydrogenation reactions of cyclohexane and acetophenone. The Pt/C and Pd/C catalysts are prepared from conservative chloride forerunners by adsorption and precipitation-deposition methods. The performance tests were carried out using a stainless bar reactor with a stirrer at 30°C . The characterization results show that the Pt/C and Pd/C catalysts gotten from the adsorption method revealed better hydrogenation activity compared with the commercial catalysts and catalysts prepared by the precipitation-disposition approach. The enhanced performance is associated with the decrease in metal crystallite sizes of Pt or Pd formed on the agitated carbon support upon the adsorption of the precursors.

Lian *et al.*, [70] investigated the influence of preparation methods on the performance of VO_x/CeO_2 catalysts for proper selective catalytic reduction of NO_x with NH_3 . VO_x/CeO_2 catalysts were prepared by homogenous precipitation method, rotary evaporation impregnation, incipient wetness impregnation, and the sol-gel method, respectively. Selective catalytic reduction activity tests were performed in a fixed-bed quartz flow reactor at atmospheric pressure. VO_x/CeO_2 prepared by simple homogenous precipitation showed higher catalytic activity and better H_2O and SO_2 resistance than catalyst prepared by other approaches. It attributed to the minimal content of CeO_2 crystallinity on the surface, better dispersion of vanadium species, and higher surface concentration of vanadium species, with the inclusion of more acid sites. Guo *et al.*, [71] researched on the effects of impregnation methods (co-impregnation and sequential impregnation), and mode of drying (air and vacuum) on the structural and catalytic behaviour of MCM-41- Ni-W supported catalysts. The catalysts were used for hydrodenitrogenation (HDN) of quinolone between $300\text{--}400^\circ\text{C}$. The results proved that the catalysts synthesised by sequential impregnation and vacuum dried synthesised

catalysts were better than the air-dried incentives. This deduction is based on the level of dispersion, active phases formation, and the level of acidic sites formation on the catalysts.

2.3.2.5 Influence of choice of solvent on the heterogeneous catalyst performance

Solvent properties like polarity, hydrogen-bond donating ability (periodicity), and hydrogen-bond accepting ability (basicity) are part of detecting factors for the performance of a catalyst. It is essential to select a suitable solvent or to verify the influence of solution in catalyst synthesis [72]. Wang *et al.*, [73] investigated the solvent effects on the preparation of Pd-based catalysts prepared by a facile solvothermal method. Pd/XC-72 catalysts were prepared as Pd/XC-72(EA) using ethanol, Pd/XC-72(EG) using ethylene glycol, and Pd/XC-72(GI) using glycerine as several solvents. After testing the catalysts for solvent-free selective oxidation of benzyl alcohol, it was discovered that Pd/XC-72(GI) had the excellent metallic dispersion and micropore size of 4.9nm. This was attributed to its unique catalytic performance for solvent-free selective oxidation of benzyl alcohol.

Zou *et al.*, [74] investigated the influence of the solvent used to synthesize Co-B alloy on its catalytic attributes like specific surface area, morphology, composition, crystallinity, and reducibility of the alloy particles. The solvents employed for the catalyst synthesis were acetone, methanol, water, and acetonitrile, respectively. The hydrogen generation assessed the catalytic performances of various Co-B catalysts during the hydrolysis of NaBH₄ (1.5%) at 298K. The Co-B in acetone showed outstanding catalytic performance, designated by a hydrogen formation rate of 5733 mL.min⁻¹.g⁻¹ during the hydrolysis though acetonitrile had the highest surface area of the alloy particles. The most inferior catalytic performance for the hydrolysis of NaBH₄ due to the oxidation of the particles in the air [75].

2.3.2.6 Influence of calcination temperature on the heterogeneous catalyst performance

Nayebzadeh *et al.*, [76] investigated the influence of calcination temperature on the catalytic performance of prepared SrO/S-ZrO₂ by solvent-free method for esterification of oleic acid. The calcination temperatures employed for the preparation of SrO/S-ZrO₂ catalysts were 400, 500, 600, 700, and 900°C, respectively. With characterization and catalysts testing, the catalyst Sr-promoted sulphated zirconia at 500°C exhibits the highest activity and part of the tetragonal phases of zirconia. It converted 91.13% of oleic acid to fatty acids methyl esters (FAME) in the esterification reaction. Amadine *et al.*, [77] studied the influence of calcination temperature on the structure and catalytic activity of copper-ceria mixed oxide catalysts in phenol hydroxylation. The CuO/CeO₂ supported catalysts were synthesised by the surfactant-template approach and calcined at temperatures between 400-800°C for 12h under flowing air. The catalytic phenol hydroxylation reaction was carried out in thermo-stated. The reactor designed with a magnetic stirrer and a reflux condenser, the catalyst calcined at 800°C had the outstanding phenol conversion, exhibited excellent catalytic stability, and selectivity for hydroquinone and catechol. That was attributed to the better electronic exchange between the two redox pairs Cu⁺/Cu²⁺ and Ce³⁺/Ce⁴⁺, and the lattice oxygen induced by Cu-O-Ce solid solution in CuO-CeO₂ supported catalyst.

Sistani *et al.*, [78] investigated the influence of calcination temperature on the structure and activity of mesoporous CaO/TiO₂-ZrO₂ catalyst synthesized by sol-gel technique for esterification reaction. The synthesized catalysts were calcined at various temperatures in the range of 100-500°C for 4h at ambient air. The activities of the synthesized enzymes were carried out in 100cm³ stainless steel reactor provided with thermocouple (Type K) and manometer at 150°C for 4h with a constant stirring speed of 600 rpm. It was discovered that the sample calcined at 400°C showed the unusual

catalytic activity that converted 86.2% of oleic acid to ester, due to its uniform particles with uniform size. The stability tests on the catalyst indicated that the nanocatalyst could maintain its performance for at least five runs.

It is increasing the calcination temperature results in an increase in the average particle size of a catalyst. Also, grain boundaries expand, and the attendant increase in particle size is due to an increase in the calcination temperature [79]. As established, the introduction of zirconia in cerium-based materials through high-temperature calcination can improve the thermal resistance and dispersion of the active component on the support, which by extension, improve the performance of the catalysts [80]. The calcination temperature is severally reported that it has a significant influence on the crystallite size, surface area, degree of dispersion, and catalytic activity of catalysts.

2.3.2.7 Influence of drying temperature on the heterogeneous catalyst performance

Guo *et al.*, [81] studied the influence of drying conditions on the preparation of the catalyst, and they deduced that it had a significant impact on the based metal species, which is vital in catalyst synthesis. Vacuum condition is discovered to be useful for maintaining the order structure of the catalysts. Albretsen *et al.*, [82] investigated the influence of drying temperature on iron Fischer-Tropsch catalysts synthesised by solvent deficient precipitation. In the preparation of enzyme, all the precursors except one were first dried in the preheated oven at 60°C for 16h, followed by a 6h final dry at 80, 100, 115, 139°C at a ramp rate of 3°C/min in 100-200cm³/min of flowing air. In contrast, the isolated catalyst was dried for 8h at 150°C as the final drying temperature. The terminology used for the enzymes was based on their final drying temperature, and the catalyst prepared without pre-dry was designated with suffix NP, meaning not pre-dry.

Fischer-Tropsch synthesis rate data were gotten during test reaction in a fixed-bed reactor at defined conditions, after due catalyst characterization. It was discovered that catalysts synthesized by the solvent deficient precipitation technique and dried at 130°C have better pore volume, surface area, the extent of reduction. Therefore, Fischer-Tropsch rate and more inadequate methane selectivity compared to other catalysts prepared at lower or higher temperatures. This is ascribed to the significant Fe⁰ availability in the catalyst dried at 130°C.

2.3.2.8 Influence of metal loading on the heterogeneous catalyst performance

Metal loading has a vital influence on the particle size and dispersion of the catalyst on the support, which invariably has effects on the catalyst's performance and selectivity. Saud *et al.*, [83] reported the impact of low metal charging palladium mixed-oxides catalyst for the preparation of glycerol carbonate using sol-gel and impregnation, respectively. The palladium was respectively loaded with SnO₂ and ZnO to synthesize Pd-SnO₂ and Pd-ZnO for the catalytic reaction. The catalytic performances conducted in a reactor at a temperature of 150°C under atmospheric pressure after the initial conditioning of the reactor. It was discovered that PdZnO has higher catalytic activity over PdSnO₂ due to its basicity property. Also, the selectivity and yield results obtained from the palladium zinc oxide catalyst synthesised by sol-gel are better compared to the catalyst manufactured through the impregnation technique. This is attributed to the amount of Pd present in each catalyst and the attribute of ZnO. Thus, the catalytic performance comparison is made based on turn over frequency (TOF) on a mole of Pd metal. Hassan and Hameed [84] investigated the Fenton-like decolourization of an Azo dye, Acid Red 1(AR1) by Fe-ball clay (Fe-BC) catalyst, with emphasis on the effect of initial iron ions loading on ball clay. The catalyst dosage, initial concentration of reactants, reaction temperature and initial solution pH on the decolourization of AR1 were also investigated. The

heterogeneous Fenton oxidation results depicted that the increase in iron-ion loading on the BC leads to the rise in decolourisation rate, and 99% decolourization was achieved for 1.0wt% within 180 min. Increasing the base metal loading results in blockage of pore and agglomeration of the metal particles, and these combined effects result in a metal reduction in the BET surface area and total pore volume.

2.3.2.9 Influence of pH on the heterogeneous catalyst performance

The dissociation of hydrogen peroxide (H_2O_2) in the presence of 0.333g/L of manganese oxide (MnO_2) catalyst was studied at a pH range of 3-10 in aqueous solution at 30°C. The pH of the solution mixture was altered by dilute solutions of hydrochloric acid (HCl) and ammonium hydroxide (NH_4OH). The result showed that the decomposition of H_2O_2 was measurable at the pH values above the point of zero charges (PZC) and increased with the increases in pH. Whereas at the pH values less than PZC, the decomposition was noticeable. As such, it was only the harmful surface sites that were catalytically active for the dissociation of H_2O_2 , and the positive surface sites were passive [85]. A zeta potential measurement is used to evaluate the solid/liquid interfacial charge processes and mingling between particulate surfaces. With Zeta potential measurement, it can be deduced the transition exhibits by a catalyst from the positive potential at low pH to the negative potential at high pH. It was confirmed that variation in pH results in the changes in the surface area (defect structure), which are considered to be the determinant for the changes in the catalytic attributes of most nanoparticles [86]. The effect of the initial pH solution on the activity of Fe-BC catalyst to decolourize AR1 was studied by varying pH in the range of 2-5. The results showed that the highest pH for decolourization of AR1 was obtained at pH3 with 99% decolourization efficiency within 180min reaction time [87].

2.3.3 Steps involved in the heterogeneous catalysis

Catalysis aided with solid catalysts takes place when the reactant molecules adsorb with the active sites, which are domiciled inside the catalyst pores. It implies that reactant molecules move via fluid layer revolving the catalyst particles (external diffusion), then through the orifice inside the particle (internal diffusion). The domestic distribution of the molecules struggles with the reaction; at the same time, the external mass transfer is influenced by the stagnant film thickness and the activity on the outer layer. The typical and conventional seven steps for a heterogeneous catalytic reaction as shown in Figure 2 are (1) movement of the reactants from the bulk phase (boundary layer) to the external surface of the solid catalyst (film diffusion or interphase diffusion). (2) Movement of the reactant from the pore mouth through the catalyst pores to the closer internal catalytic surface. The point where the chemical transformation takes place, (pore diffusion or intra-particle diffusion), (3) adsorption of reactants on the inner catalytic surface, (4) catalytic surface reaction active sites, (5) desorption of the products from the inner surface, (6) movement of the products from the interior of the solid catalyst to the pore mouth at the external surface, and (7) movement of the products from the outer pellet surface to the bulk fluid (interphase diffusion).

2.3.4 Diffusion phenomenon in catalysis

Diffusion of fluid mixtures within a porous matrix is frequent and vital in catalysis, adsorption, and membrane separations. In general, there are three types of diffusion mechanism as relates to catalysis. These are bulk diffusion, Knudsen diffusion, and surface diffusion, as shown in Figure 3. (i) Bulk diffusion: It is said to occur when the pore size is immensely larger compared to the mean free

path of the diffusing molecules. It is prominent for large pore size and high system pressure. Molecule-molecule collision dominates over molecule-wall clashes, in this type of diffusion. (ii) Knudsen diffusion: This occurs if the pore diameter is the same as the mean free path; the diffusing molecules hit the pore walls more often than the other particles. It turns overwhelming if the mean free path of the molecular species is significantly larger than the pore diameter, and in turn, molecule-wall collision becomes essential. Diffusion is usually in the Knudsen regime when the average pore radius is less than 100nm. (iii) Surface diffusion: It takes place when the pore diameter of microporous solid is almost the same size as the reactant molecule, the reactant molecules usually move within the pores, in such that it maintains contact with the pore walls. In surface diffusion of adsorbed molecular species via the pore wall surface, the pathway of the species becomes dominant for micropores and adhesively attached species [89].

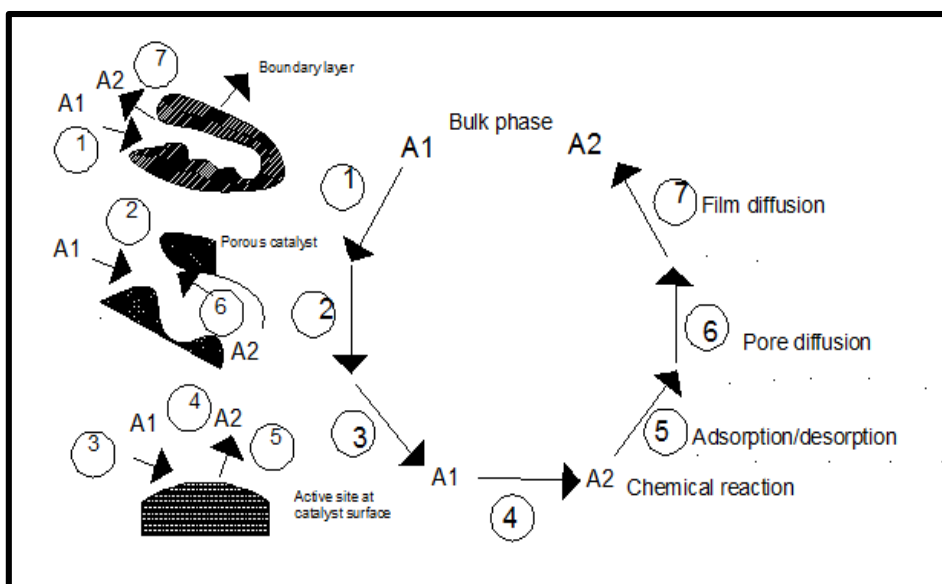


Fig. 2. Diagram of catalytic heterogeneous reaction mechanism [88]

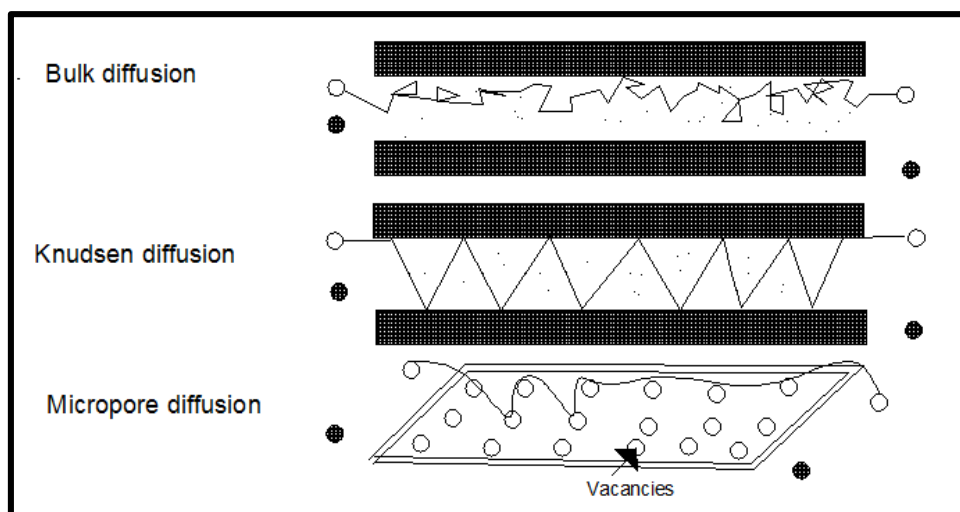


Fig. 3. Prevalent mechanisms at which molecular species move inside a solid catalyst

2.4 Heat and Mass Movement Limitations during Solid Catalyst Aided Reaction

Heat and mass transfer is very significant in determining the rate of heterogeneous catalytic reactions. Heat transfer limitations involve the verification of the nature of the response, whether it is isothermal or not, and to determine the maximum temperature within the catalyst particle at which reaction is taking place. The heat generation rate is dependent on the reaction rate, and the rate of reaction is temperature-dependent under Arrhenius law. Using a tubular reactor increases the temperature along the reactor length for an exothermic reaction, except there is an effective cooling system. The temperature at a point closer to the tube axis is significantly higher than points close to the tube wall. Summarily, the temperature is significant in the design of a reactor, given reaction rate sensitivity to heat [90]. Mass transfer limitations involve diffusion of components (both internal and external) to and from the solid catalysts.

During a catalysed reaction, the reactants must move from the solid catalyst external surface to the metal particles through the pellet porosity. This mechanism is often responsible for mass transfer diffusional limitations during the reaction [91]. The rate of heterogeneous catalytic response reduces with the time-on-stream as a result of catalyst ineffectiveness. The product or by-product formed during the catalytic reaction usually cover the catalyst pores, which, in turn, confine the mass transfer process from the external pore mouth to the internal catalyst surface [92]. Diffusional confinement can be discouraged by using powdered catalyst instead of pellets; this reduces the mean distance between the reactant flow and the metal particles. However, in the case of a packed bed reactor, it is not advisable because of the tremendous pressure drop challenges. The catalyst with a pore diameter of less than 100nm, the diffusion phenomenon in the pores depends on both the ordinary gas diffusion and the Knudsen diffusion.

2.4.1 Internal diffusion influence on heterogeneous catalysis

Pores contain in solid catalysts contribute to its increase in surface area for adsorption and reaction. Mostly, pore network in highly porous solids house the catalytically active sites, and the diffusion of molecules in restricted locations is very vital in the observed rate of reaction determination. However, the mean free path of gases is usually more than the dimensions of small pores typical of solid catalysts. In the case of Knudsen diffusion, where microspores of solid catalyst are more than mean free path of gases, the collision of molecules with the pore walls is more than with other molecules. The Knudsen diffusivity of component A, D_{ka} , is proportional to $T^{\frac{1}{2}}$, and is not dependent on pressure and the presence of other species [93].

$$D_{ka} = 9.7 \times 10^3 R_{pore} \left(\frac{T}{M_A} \right)^{\frac{1}{2}} \text{ cm}^2/\text{s} \quad (8)$$

where R_{pore} represents the pore radius in cm, T represents the absolute temperature in Kelvin, and M_A represents the molecular weight of A.

Based on mole balance for diffusion and reaction inside the solid catalyst as described by Fick's law, the internal diffusion rate, N_A (mol/cm²s) is defined as:

$$N_A = -D_e \left(\frac{\partial c_A}{\partial z} \right) \quad (9)$$

where C_A represents the number of moles of component A per unit of the open pore volume, z represents the diffusion coordinate and D_e describes the effective diffusion coefficient (cm^2/s).

Transport phenomena cannot be described with either molecular or Knudsen diffusivity if both molecule-molecule and molecule-wall collisions are vital. In the case of equimolar counter diffusion of a binary mixture, the diffusivity of component A, D_{TA} , can be evaluated by the Bosanquet equation.

$$\frac{1}{D_{TA}} = \frac{1}{D_{AB}} + \frac{1}{D_{ka}} = \frac{1}{D_{AB}} + \frac{1}{9.7 \times 10^3 R_{pore} \left(\frac{T}{M_A}\right)^{\frac{1}{2}}} \quad (10)$$

where D_{AB} represents the molecular diffusivity, D_{ka} represents the Knudsen diffusivity, R_{pore} represents the pore size, T represents the temperature, and M_A represents the molecular mass of the diffusing species.

2.4.2 Effects of external transport on heterogeneous catalysis

Reaction aided with solid catalysts can only happen if the reactant can diffuse through the stagnant boundary layer surrounding the catalyst particle. There is a limitation of the Fick's law in describing diffusion, especially a multicomponent system. Maxwell-Stefan formulation has been reported as a convenient method to describe mass transport regarding the inventory of thermodynamic non-dualities and influence of external force fields. Several factors that could be used to determine the overall rate of heterogeneous catalytic reactions are reaction kinetics, the effect of adsorption, desorption, internal diffusion and external diffusion of reactants and products. Turbulence within the reaction mixture influences the diffusion of reactants and products in the bulk fluid outside the solid catalyst particle. It is necessary to determine the actual catalyst size required to discard the diffusion control limitations in the heterogeneous catalytic reaction, being a prerequisite to obtaining exact reaction kinetics. The particle size is determined by applying the Weisz-Prater criterion [94].

2.4.3 Weisz-Prater criterion

The effective diffusivity in the pores is used to determine the Weisz-Prater parameter (ϕ_{WP}). The effective diffusivity of reactants in the gas phase is quickly evaluated, using molecular or Knudsen diffusion depending on the proportion between the mean free path (λ) and the average pore diameter (d). The observed reaction rate is cardinal in the assessment of internal transport limitations via the Weisz-Prater criterion. Weisz-Prater parameter (ϕ_{WP}) is expressed as the ratio of the rate of reaction (r_A in mole/ cm^3s) to the internal transport rate, as presented in Eq. (11).

$$\phi_{WP} = \frac{r_A R_p^2}{C_{S,A} D_{eff}} \quad (11)$$

where R_p represents the radius of the catalyst particle, in cm, $C_{S,A}$ represents the concentration of A at the external surface, in mol/ cm^3 , and D_{eff} describes the effective diffusivity of A, in cm^2/s .

The critical value of ϕ_{WP} lies on the value of reaction order. The critical value for zero order, first order, and second-order are 0.3, 0.6, and 6, respectively. It implies that limited diffusion reactions have $\phi_{WP} > 6$, while transport limitation is absence and concentration gradient does not exist within the solid catalyst, if $\phi_{WP} < 0.3$. Weisz-Prater parameter (ϕ_{WP}) can equally be defined in terms of Thiele modulus and the internal effectiveness factor according to

$$\phi_{WP} = \eta \phi_n^2 \quad (12)$$

where η represents the internal effectiveness factor and ϕ_n represents the Thiele modulus.

Thiele Modulus and effectiveness factors are used to determine the suitable particle size that can avoid internal diffusion limitation [95].

2.4.4 Effectiveness factor

The effectiveness factor (η) measures how fast the reactant diffuses into the solid catalyst before the product is formed. In other words, the effectiveness factor is used to elucidate the effect of mass transfer resistances inside the catalyst particle. The catalyst shape and reaction order is used to determine the effectiveness factor. It is the ratio of diffusion rate to the reaction rate without any diffusional (internal transfer) limitations. Thus, the value of η varies between 0 and 1. Effectiveness factor can be calculated for the n th reaction order as

$$\eta = \left(\frac{2}{n+1} \right)^{\frac{1}{2}} \frac{3}{\phi_n} \quad (13)$$

where n represents the order of the reaction.

For η near unity, reaction at the entire volume of solid catalyst is high because the reactant diffuses quickly through the solid catalyst. As such, internal diffusion in the catalyst is negligible. For η near zero, the reaction is at a low rate because the reactant cannot move into the solid catalyst interior, and the reaction rate is minimal in a large volume of pellet [96]. The internal effectiveness factor, η , is equally applied to verify if internal diffusion is the rate-limiting step. Considering the first-order reaction using a spherical catalyst, to evaluate the internal effectiveness factor using expression designated with Eq. (14) [97].

$$\eta = \frac{3}{\phi_1^2} (\phi_1 \coth \phi_1 - 1) \quad (14)$$

2.4.5 Thiele Modulus

Thiele modulus (ϕ) is the ratio of surface reaction rate to diffusion rate. It is used to evaluate if catalyst activity is impeded by internal transport. If the Thiele modulus is significantly high, the mass transfer determines the reaction, and if it is low, then the surface reaction is adjudged to be the rate-limiting step. Small values of this parameter indicate little mass transfer limitations. It is expressed mathematically as

$$\phi = R \sqrt{\frac{K S_a \rho_p}{D_{eff}}} \quad (15)$$

Where R represents the radius of the diffusion path, K represents the rate constant, S_a represents the metallic surface area per gram of support, ρ_p represents the density of the support and D_{eff} describes the effective diffusivity [98].

2.5 Heterogeneous Catalyst Preparation

Solid catalyst preparation comprises of active components precursors, support, and any desired promoters and homogeneous mixing of the constituents in a suitable solvent. The precipitant formed, which could be used to either coat an inert carrier or to impregnate on a carrier. The dried product is mixed with either a binder or forming agent, then grind, pelletized, and shaped. The final product is calcined and activated by either oxidation or reduction or both. Prominent factors that catalytic activity of a catalyst lies on particle size, nature of oxide support, surface area, and the electronic configuration of its specific sites. Hence, the method of preparation has a vital role in the precursor structure of the catalyst and its activity [99] [100].

Hydrothermal method: A hydrothermal synthesis is an approach of synthesizing single crystals which depends on minerals' solubility in hot water at elevated pressure. The technique supplies a suitable morphology orientation [101]. It is a chemical-based technique conducted at low temperatures to produce high surface area nanometric powders, marginal size distribution, and crystals with perfection devoid of the need for subsequent thermal treatments [102].

Precipitation method: Precipitation is a form of crystallization approach which takes place using the bulk of the liquid or via a relatively inert surface, where the support act as crystallization nuclei for the active site precursor. **Co-precipitation method:** This procedure is centred on the amalgamation of aqueous phase metal salts and alkali solutions to produce a dissolvable metal hydroxide or carbonate. The precipitation procedure can be induced by a change in surroundings such as temperature, actual value, and rate of pH value, evaporation, and attentiveness of salt. These parameters carried about progressive changes in crystal growth and their aggregation [103]. Co-precipitation leads to a well-defined and crystalline precursor component with a mixed cationic lattice that contains all metal species of the final catalyst. The gain of this technique is that it offers better size control. This size control is achieved by mixing a precipitating agent to the solution of precursor [104].

Sol-gel method: The sol-gel technique is suitable for the synthesis of metal nanoparticles embedded with oxide matrix with marginal particle size distributions and adjustable metal loadings [105]. This method permits the control of texture, constituents, uniformity, and structural attributes of solids, and it makes catalyst production possible and chemically modified supports. It is a synthetic approach for the preparation of amorphous as well structurally ordered materials, where the properties (i.e., porosity and surface area) of the synthesized samples can be regulated to obtain homogenous matrices [106]. **Solvothermal method:** In the solvothermal process, particles are formed in an organic solvent or water at a temperature above the boiling point of solvent and pressure above vapour of solvent, to alleviate the interaction of precursors during preparation. Using water as a solvent is referred to as hydrothermal synthesis. The prominent properties governing solvothermal reactions are (i) chemical parameters like the nature of the reagents and environment of the solvent (ii) thermo-dynamical parameters like temperature, pressure, and the reaction time [107]. The solvothermal method is secure, and it avails the possibility of controlling the shape and size distribution, crystalline of the desired product via regulating properties like time of the reaction, the temperature of the response, solvent nature, nature of surfactant and the nature of precursor. However, it is associated with safety challenges, as it is impossible to observe the reaction process [108]

Impregnation method: In the impregnation technique, support is contacted with the impregnation solution for a designated time, dried to remove the imbibed liquid, and calcined. The method is known as incipient if the solution volume impregnation as the same pore capacity of the support. The impregnation method is suitable to prepare supported metal catalysts and mixed

catalysts preparation [109]. Guo *et al.*, [71] reported that indices like structure, dispersion, and chemical states of prepared catalyst and its activity are influenced by impregnation technique. Petkovic and Ginosar [104] indicated that catalyst synthesis by impregnation method display high activity and short initial induction period. Table 1 shows the results of different authors on the conversion of ethanol over catalysts of different preparation methods, operating conditions, and the product (H₂) yield and selectivity.

Table 1

Effect of Catalyst Preparation on ethanol conversion, the product yield, and selectivity

Method of catalyst preparation	Catalyst formation	Ethanol conversion (%)	Hydrogen yield (%)	Hydrogen selectivity (%)	References
Impregnation	Ni/MgAl ₂ O ₄ -CeO ₂	90	87	80 at 650°C	[56]
Wet impregnation	Pt-Ni/CeO ₂ -SiO ₂	98	65	62.5 at 600°C	[98]
Deposition-precipitation	Ir-CeO ₂	94	72	60 at 650°C	[99]
Co-precipitation	Ni-Co-Zn-Al hydrotalcite-like	100	82	89 at 497°C	[31]
Co-precipitation	Ni/Al ₂ O ₃	85	72	91 at 600°C	[100]
Wet impregnation	Co/Al ₂ O ₃	95	38	53.7 at 400°C	[101]
Impregnation	105 La/ TiO ₂	27.5	14.8 at 500°C	55	[102]
Impregnation	3Pt/10Ni	100	45 at 300°C	44	[103]
Impregnation	Ni/Al ₂ O ₃	62	55 at 600°C	40	[104]
Impregnation	1%Rh/CeO ₂ -ZrO ₂	98	70 at 550°C	62	[105]

Synthesised catalysts are characterized to determine its properties. The most important of these is the identification of atom-type present at the catalyst surface. The second concern is the atoms oxidation state that constitutes the active phase—lastly, the determination of the level of dispersion of active ingredient over the catalyst surface.

2.6 Characterization of Heterogeneous Catalyst

Catalysts that are complex in composition, texture, and structure of the phases are referred to as heterogeneous catalysts. Generally, catalysts have specific applications, and as such, there is a need to subject them to characterization to determine their suitability. The heterogeneous catalyst characterization refers to the evaluation of its physical and chemical properties, which are determinant of its activity in a reaction. In other words, it is done to access the variation in physical and chemical attributes of the as-synthesized catalyst during synthesis, activation, and test reaction for better knowledge and quality control. Characterization gives the understanding of catalyst surface structure, texture, metal dispersion on support, morphology, and pore structure of the support. The prominent characterization techniques are Transmission Electron Microscopy (TEM), X-Ray Diffraction (XRD), Thermogravimetric Analysis (TGA), Pyridine Adsorption for Fourier Transform Infrared Spectroscopy (Py-FTIR), Temperature Programmed Desorption of Ammonia (NH₃-TPD), Scanning Electron Microscopy (SEM), Energy Dispersive X-Ray (EDX), Temperature Programmed Oxidation (TPO), Temperature Programmed Reduction (TPR) and Brunauer Emmet Teller Technique (BET). The comparative result on the fresh and spent catalyst is used for every analytical technique to illustrate for better understanding.

2.6.1 Transmission Electron Microscopy (TEM) and X-Ray Diffraction Technique (XRD)

Transmission Electron Microscopy (TEM) is an essential technique for directly imaging nanomaterials to get sizable measures of particle or grain size, morphology, and size distribution. The transmission electron microscope uses a thin specimen (ideally ≤ 100 nm) is exposed to a high-energy (typically 60 - 300 keV) electron beam. Even high technology TEM can attain a high spatial resolution of 0.05nm, with energy-resolution as high as 7mev. Images generally contain contrast that may be due to crystallinity, atomic mass, or thickness variations within the sample. Crystallographic information can also be obtained from diffraction patterns. However, because electrons are used rather than light to illuminate the sample, TEM imaging is associated with high resolution (by a factor of about 1000) compared with a light-based imaging technique, because electrons are applied instead of light-based imaging techniques as depicted in Figure 4. The three prominent TEM techniques are imaging techniques such as high-resolution TEM, scanning transmission electron microscopy (STEM) imaging, and 3D electron tomography technique. Spectroscopy techniques such as X-ray energy dispersive spectroscopy (EDS), electron energy-loss spectroscopy (EELS), and TEM-cathodoluminescence microscopy (TEM-CL); diffraction techniques (such as selected area electron diffraction (SAED), nano-beam electron diffraction (NBED), and convergent beam electron diffraction (CBED)) and their combinations are equally applicable [106]. TEM has two modes; a bright-field mode where the intensity of the transmitted beam provides a two-dimensional image of the density or width of the sample and a dark field mode where there is a record of electron diffraction pattern [107].

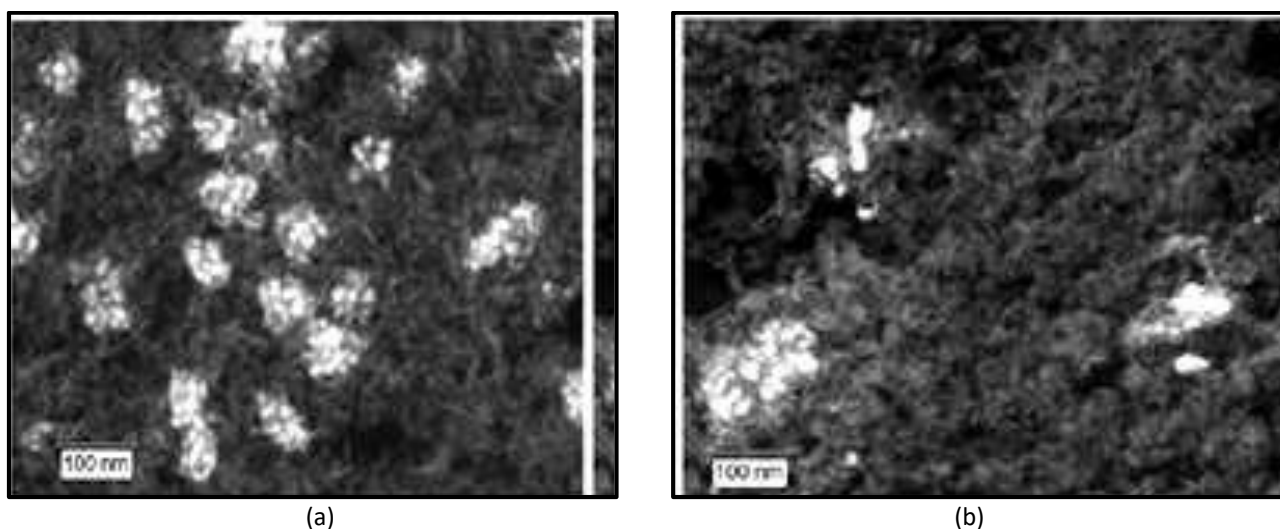


Fig. 4. TEM view of Co-alumina catalyst for Fischer-Tropsch synthesis (a) fresh (b) spent [107]

A solid could exist in various crystallographic phases, such that each stage is distinct in terms of catalytic property. X-ray diffraction is used to investigate the bulk phase constituents, degree of crystallinity, unit cell parameter, new crystalline phases of as-prepared catalyst samples. The x-ray diffraction analysis is associated with the incidence of an x-ray beam over a sample stationed on Pyrex support. As x-ray touches the sample, it diffracted at angle θ , and finally detected by a scintillation counter. XRD peaks are yielded with constructive interference resulting from a monochromatic beam of x-rays diffracted at designated angles from every set of lattice planes in a sample. The area under the peak depicts the amount of every phase present in the sample, as shown in Figure 5. The area under the peak intensity. The technique is governed by Bragg's law [108]:

$$2d_{hkl} \times \sin \theta = n\lambda \quad (16)$$

where

d_{hkl} = inter-articular distance (Å)

2θ = angle between the incident and diffracted beam (°)

n = serial diffraction order of Bragg (integer)

λ = wavelength of the beam

Relating the diffraction peaks with the d-spacing enables the identification of the mineral since every mineral has a set of specific d-spacing. Conventionally, it is done by comparing the d-spacing with standard reference patterns. For typical powder pattern, data are collected to 2θ from 5° to 70° , angles that are present in the x-ray scan.

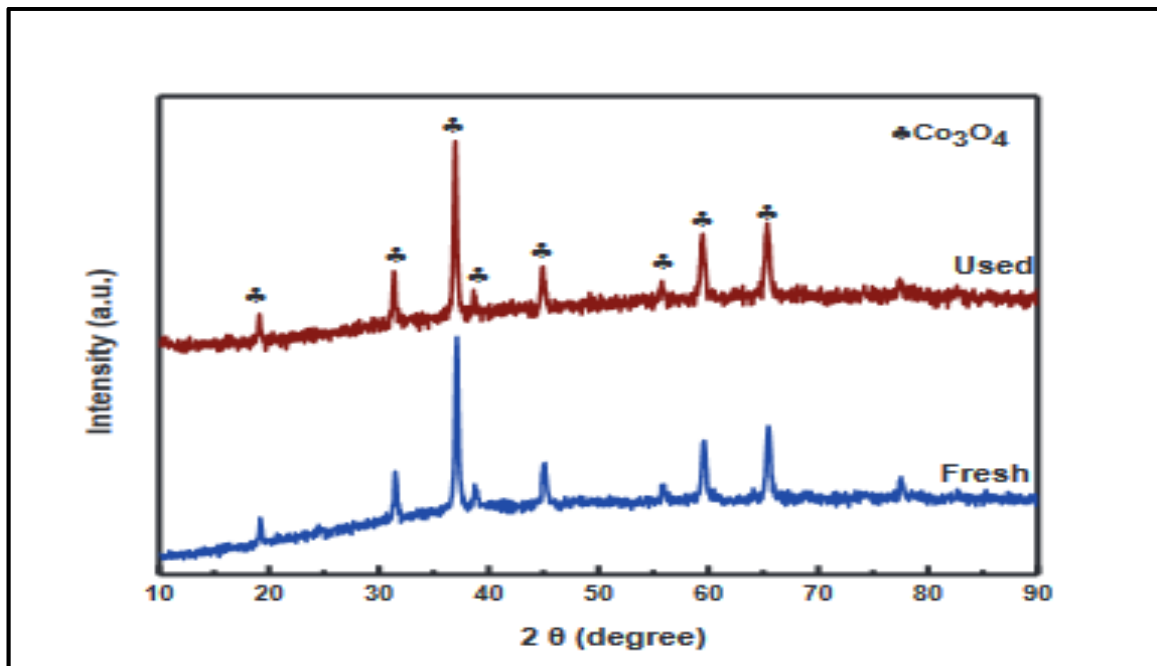


Fig. 5. XRD patterns of fresh and used 0.2%Ni/Co₃O₄(C₃) catalysts [109]

2.6.2 Temperature-programmed oxidation (TPO) and temperature-programmed reduction (TPR)

Temperature-Programmed Oxidation (TPO) is an essential tool used for the determination of the amount and the chemical state of carbon residual on the used catalysts. The first product during TPO is carbon (IV) oxide (CO₂), and a negligible amount of carbon (II) oxide (CO) is usually liberated at the same temperatures as CO₂, shown in Figure 6. This oxidisable carbon deposited on the surface generally evaluated the rationalized weighted catalyst. A stream of diluted oxygen (2-100% oxygen in helium) is focused over the sample during a linear heating ramp, which produces a signal as a result of oxygen loss from the gas stream. TPO analysis allows quantifying the oxidation capacity of the active metal catalyst. Combining TPO with TPR provides for estimating the number of regeneration cycles that an enzyme can undergo before completely deactivated [99], [110].

Temperature-Programmed Reduction (TPR) is applicable in evaluating the number of reducible species present on the surface of the catalyst. It shows the temperature associated with the reduction of every species. Hydrogen in argon is commonly used as reducing gas mixture for catalyst reduction. During the process, hydrogen consumption by adsorption/ reaction is observed, as the

sample temperature is gradually increased with time. Differences in the concentration of the gas mixture downstream from the reaction cell are recorded. It is a popular characterization technique because of its low cost, relatively simple instrumentation, and utility. The derivative of the weight change with time as a function of sample temperature is usually used to report the TPR profiles, as depicted in Figure 7 [111]. The reduction index is evaluated using Eq. (17).

$$\text{The extent of reduction} = \frac{\text{Actual amount of hydrogen consumed}}{\text{Theoretical amount of hydrogen consumed assuming complete reduction}} \quad (17)$$

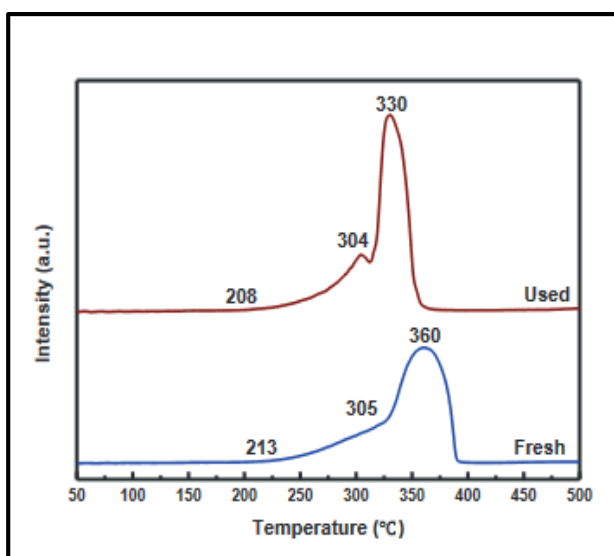


Fig. 6. TPO profile of used catalysts for CH₄-TPR [110]

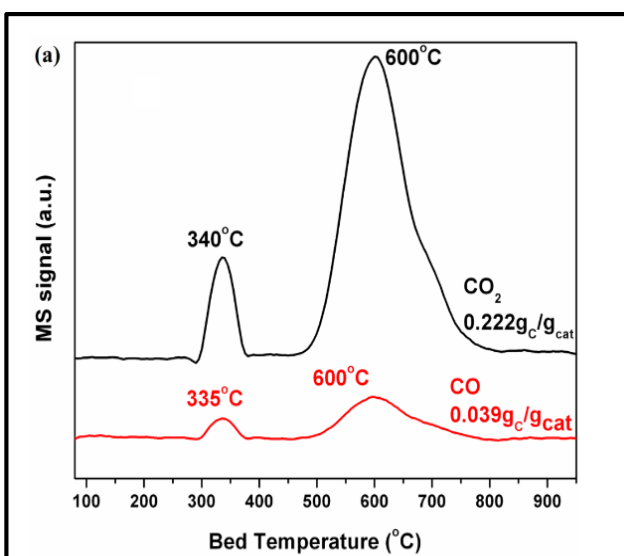


Fig. 7. TPR profiles of fresh and used 0.2%Ni/Co₃O₄(C₃) catalysts [109]

2.6.3 Thermogravimetric analysis (TGA)

Thermogravimetric analysis is useful in determining either the main gain or loss as a result of structural and state changes resulting from temperature increase of a solid substance. Because of the ability to automatically switch gases within the TG system, it is widely used to measure the total amount of accumulated coke on the catalysts. TG is also utilized to determine the decomposition kinetics, residual solvent levels, and polymer degradation temperatures. The weight loss curve from the TG instrument is used to characterize the exact point at which weight loss occurs, as illustrated in Figure 8(a) and (b). Three standard stages can be pointed out on the thermogravimetric curves when Ni-based catalysts coated with coke undergoes analysis. The first stage happens between a temperature of 0-100°C, and a mass decrease as a result of water vaporization occurs [112]. The second stage happens at around 350°C as an indication of Ni phase oxidation, and the final stage occurs at a temperature above 400°C, as an indication of carbon combustion [113]. Also, the two different types of carbon usually deposited on the catalyst's surface are amorphous and filamentous carbon. The oxidation of amorphous carbon is estimated to begin at a temperature of 500°C, while the oxidation of filamentous carbon is usually observed at a temperature around 600°C [114].

2.6.4 Fourier transform infrared spectroscopy (FTIR)

Fourier transform infrared spectroscopy is a technique based on the vibrations of the molecules. FTIR operates based on functional groups, and peaks are used to provide the information, as depicted in Figure 9. The sample is associated with infra-red radiation, ranging between 400-4000 cm⁻¹(that

relates to the geometry of the molecule and its symmetry. FTIR consist of a moving mirror, fixed mirror, beam splitter, Infrared radiation source, and detector. However, FTIR of the pyridine (C_5H_5N) adsorbed is used to evaluate the Bronsted/Lewis acid site ratios. The formation of characteristic absorption bands is due to the vibration of pyridine (ring deformation mode), which interacts differently with these two adsorption sites. For the determination of the type of hydroxyl groups, the sample should be dehydrated at elevated temperature under vacuum pressure. Fourier Transform (FT) operates on time-domain spectroscopy, radiant power data is noticed concerning time [116].

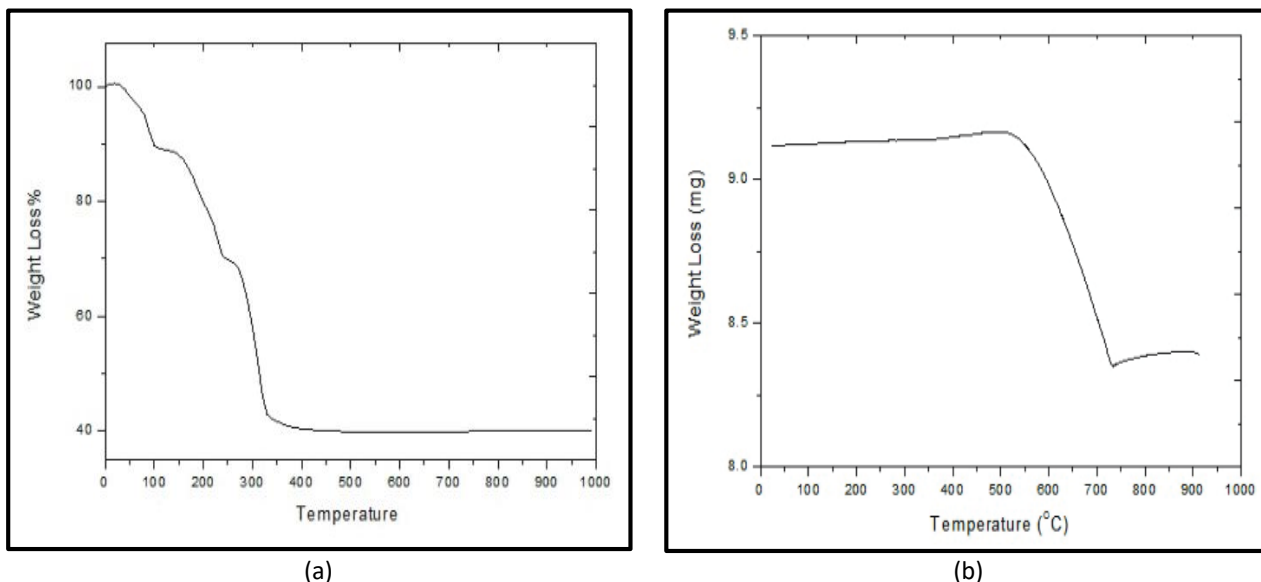


Fig. 8. TGA of Ni/Al₂O₃ catalysts (a) fresh impetus (b) used catalyst [115]

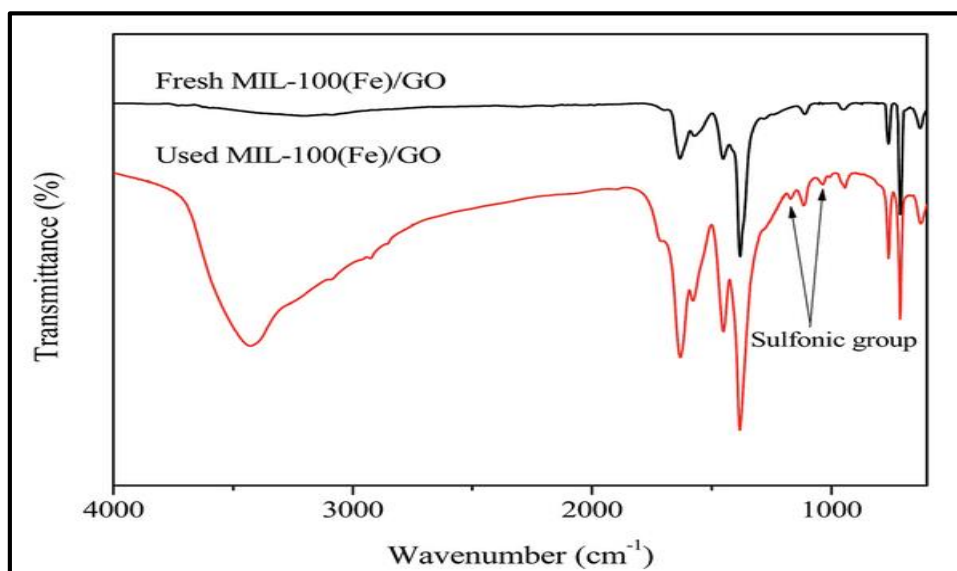


Fig. 9. FTIR spectra of fresh and used MIL-100(Fe)/GO composites [117]

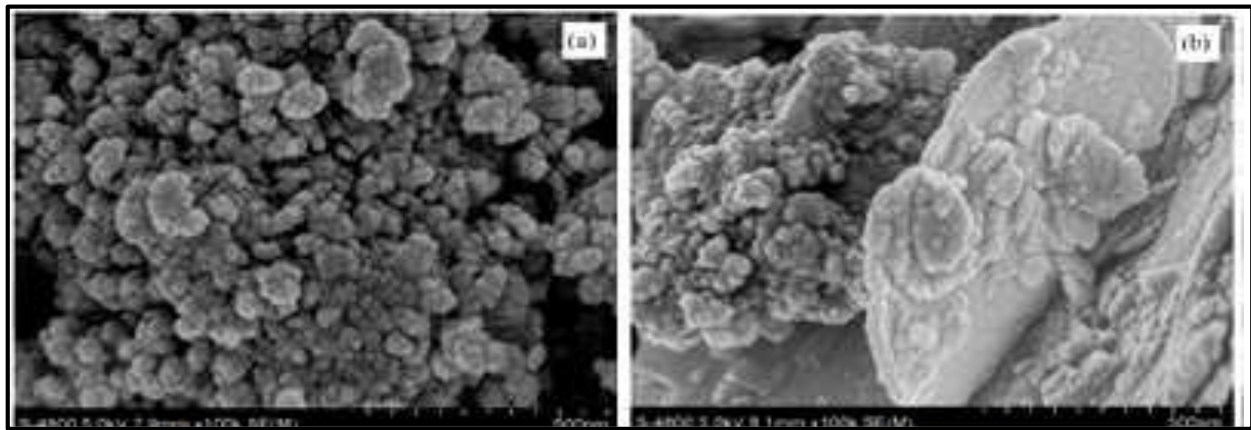
2.6.5 Scanning electron microscopy (SEM)

Scanning electron microscopy applies a directed beam of high-energy electrons to render high resolution, three-dimensional images. These images from interactions of electron-sample unveil information such as texture, chemical constituents, and crystalline structure and constituent material that the sample is made. The microscope column in this tool consists of three chambers; the electron

gun chamber, the electron beam condenser chamber, and finally, the sample chamber. The detector is utilized to transfer the secondary electrons to the cathode ray tube (CRT), which can be converted into voltage and then transformed into an image displaying the topography of the sample on an SEM screen that can be typically showed [106]. A typical example of an SEM image is, as shown in Figure 10. The expression for the magnification of SEM is

$$\text{Mag.} = \frac{W_c}{W_e} \quad (18)$$

where Mag is the magnification, W_c is the width of the CRT, and W_e is known as the width of the electron beam.



Fresh Catalyst Deactivated Catalyst
Fig. 10. SEM images of fresh and used of de-NO_x catalyst V₂O₅-WO₃/TiO₂ [118]

2.6.6 Brunauer emmet teller technique (BET)

Brunauer emmet teller (BET) technique is useful in the determination of specific surface area, pore-volume, and pore diameter of solid catalysts. In the surface of solid catalysts, noticeable defects and different pore sizes are present that are responsible for the increase in the contact area of the enzyme with the reactant. The number of pores present in the catalyst surface determines its specific surface area. The more the orifice, the larger the particular surface area. The comparative BET results of fresh and spent catalyst are presented in Table 2. However, when there is crystallized agglomerate, the surface area of the catalyst decreases. As such, support with high specific surface area provides a high distribution of the active phase [119]. The BET formula relates the volume absorbed at a designated partial pressure with the volume adsorbed at monolayer coverage. BET formula is as presented in Eq. (19).

$$\frac{V}{V_m} = \frac{C\left(\frac{P}{P_0}\right)}{\left(1-\frac{P}{P_0}\right)\left(1-\frac{P}{P_0}+C\left(\frac{P}{P_0}\right)\right)} \quad (19)$$

On linearizing Eq. (20), it becomes

$$\frac{1}{V\left[\left(\frac{P}{P_0}\right)-1\right]} = \frac{1}{V_m C} + \frac{C-1}{V_m C} \left(\frac{P}{P_0}\right) \quad (20)$$

where P and P_0 represent the equilibrium and the saturation pressure of adsorbates at the temperature of adsorption, V represents the adsorbed gas quantity and V_m represents the monolayer adsorbed gas quantity. C represents BET constant given as

$$C = \exp \left(\frac{E_1 - E_L}{RT} \right) \quad (21)$$

where E_1 represents the heat of adsorption for the first layer and E_L represents that for the second and higher layers and is equal to the heat of liquefaction, R represents the ideal gas constant, and T is the absolute temperature.

The specific surface area (S) is determined using Eq. (22), after deducting the value of V_m from the plot of $\frac{1}{V \left[\left(\frac{P}{P_0} \right) - 1 \right]}$ versus $\left(\frac{P}{P_0} \right)$.

$$S = a \frac{V_m N_A}{V} \quad (22)$$

where a represents the adsorption cross-section of the adsorbing species, V represents the molar volume of the adsorbent gas, and N_A represents the Avogadro's constant.

Table 2

Surface area determination by BET for fresh and spent catalyst

Catalyst	Surface area for fresh catalysts (m ² /g)	Surface area for spent catalyst (m ² /g)	References
Ni623	100	89	[121]
H-ZSM-22	217	27	[122]
Au/Fe ₂ O ₃ -S	47	31	[123]
Au/Fe ₂ O ₃ -W	38.7	31	[124]
5%WTPt-1%wtSn/ γ -Al ₂ O ₃	184	161	[125]
MCM-41-S1	901	464	[126]
SBA-15-S1	860	771	[127]
Sb(2%)/V ₂ O ₅ /TiO ₂	89	62	[128]
W(10%)/V ₂ O ₅ /TiO ₂	85	45	[129]
10wt%Pd(OH ₂)/C	810.9	124	[130]
Cu/ZSM-5	260	135	[132]
Ni/ZSM-5	240	120	[133]
Commercial FCC catalyst	160	70	[134]

2.6.7 Temperature programmed desorption of ammonia (NH₃-TPD)

This method is applicable in measurement of the number and base strengths of sites found on solid base catalysts. In this method, mass spectrometry is used to monitor the number of desorbed molecules, and the surface interactions are viewed with infrared spectroscopy. Using energetic bound probe molecules with high binding energies will increase in temperatures as necessary to desorb these adsorbates. The heat associated with desorption is an indication of the strength of adsorption. In contrast, the quantity of gas consumed or the amount of desorption upon heating indicates the concentration of the surface sites. Temperature programmed desorption of ammonia is useful in the determination of the number of acid sites in the catalyst. Usually, the TPD curve consists of two peaks, as shown in Figure 11. However, a low temperature (LT) can be used to represent the desorption of ammonia from the weak acid sites (i.e. physisorbed ammonia). Also, a high-temperature peak (HT) can be used to describe the desorption of ammonia molecules from the

strong acid sites (i.e., protonic acidity or chemisorbed ammonia) [134]. The prevalent molecules used in TPD are NH_3 and CO_2 as probes for acidic and basic sites, respectively. Also, experiments with pyridine, O_2 , H_2 , CO , H_2O , and other molecules are often performed as well [110].

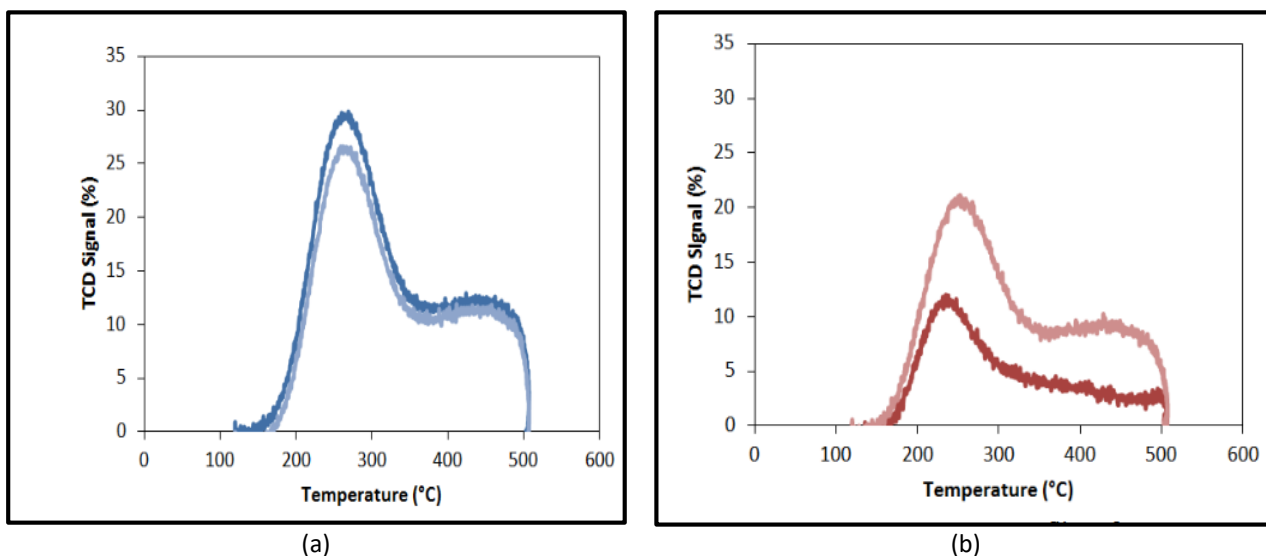


Fig. 11. NH_3 -TPD profiles of ZSM-5 for weak and strong acid sites (a) fresh (b) used [134]

2.6.8 Energy dispersive X-ray spectroscopy (EDX)

Energy dispersive x-ray spectroscopy is an analytical technique that provides information about an elemental constituent of an analyst. EDX is applicable in distinguishing between metals and various polymeric materials with specific elemental footprint. It uses the x-ray spectrum resulting from solid sample bombarded with a focused beam of electrons and results in localized chemical analysis. Qualitative analysis centres on spectrum lines identification, which is almost straight forward due to x-ray spectra orderliness. Quantitative analysis (concentrations of the determination of the elements) is carried out by comparing the line intensities of every component of a sample with of the same parts in standard form (known concentration) [135]. A typical analytical result of EDX is, as shown in Figure 12. During usage, most catalysts are deactivated at elevated temperatures and in extreme gas conditions. As such, there is a need to explain the catalyst decay mechanisms which are prevalent in chemical, petrochemical, agrochemical, and pharmaceutical industries.

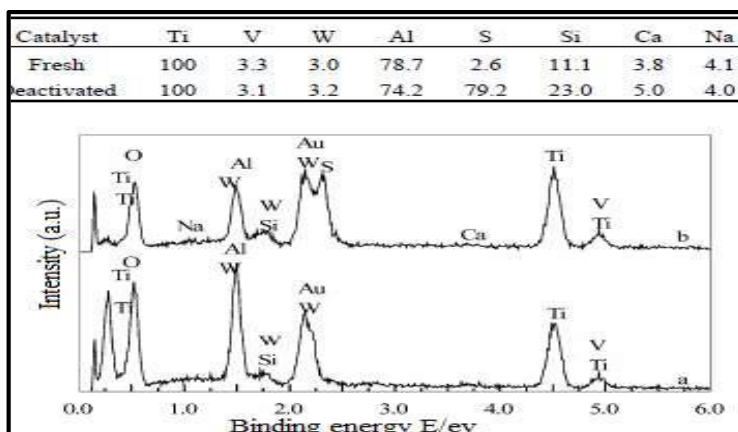


Fig. 12. EDX spectra of $\text{V}_2\text{O}_5\text{-WO}_3/\text{TiO}_2$ catalyst (a) fresh catalyst (b) deactivated catalyst [121]

3. Deactivation of Heterogeneous Catalysts

Deactivation reduces the activity of the catalyst or hinders the selectivity towards the desired products, and the level of deactivation lies on the nature of the enzyme and reforming process conditions. The economic implication of catalyst deactivation is that it adds to operating costs due to replacement or regeneration of the spent catalysts. However, deactivation of catalyst can be prevented by studying the deactivation mechanism and design of durable catalyst system. Heterogeneous catalysts deactivation is classified by type (chemical, thermal, and mechanical) and by mechanism (poisoning, fouling, thermal degradation, vapour formation, and attrition/crushing) [136].

3.1 Sintering and Coking or Fouling

Sintering is defined as catalytic ineffectiveness due to reduced active surface area resulting from a clumping together of the energetic metal particles due to prolonged exposure to excessive heat. Good knowledge of sintering mechanism is vital, both for the determination of the extent of deactivation by sintering and for the design of highly active catalysts. Sintering is bounded by factors like time, temperature, chemical environment, catalyst composition and structure, and support morphology. Since the pores catalysts are closed; as a result, the number of active sites decreases, as shown in Figure 13.

The prominent mechanisms of sintering of metal crystallite or particle growth are classified into: (i) atomic migration model (Ostwald ripening). The sintering is as a result of atomic or molecular migration over the surface of catalyst upon collision with the immovable metal crystallites yielding particle growth in place of van der Waals forces. (ii) Crystallite migration model, the sintering is said to occur when metal crystallites migrate over the catalyst surface upon collision and fusion of metal particles resulting in particle growth formation of the new compound via metal-support interaction. These mechanisms lie on the movement of the particles. The first model favours the grain growth or agglomeration in the bulk catalysts, and both the first and second models are observed in the case of supported catalysts. (iii) Vapour transport between particles (at high temperatures) [137-138]. A solid-state transformation is an advanced form of sintering that occurs at high temperatures and eventually causes the change of one crystalline phase into a different one. Sintering can be prevented by regulating the temperature of reaction and through avoidance of water and other substances that trigger metal migration.

Coking occurs as a result of carbonaceous particles being deposited on the catalyst surface, due to reactions involving unburnt hydrocarbons. With the higher accumulation of carbon deposit, catalyst effectiveness starts to decrease, as a result of obstruction of the active sites and pores, as shown in Figure 14. This obstructs the movement of reacting molecules from the bulk fluid outside the catalyst to the active sites catalyst pellets, thereby reducing the yield of the product. Fouling can be prevented by choosing a suitable operating condition that could minimize carbon formation. Carbon formation minimization is also a function of the support. The risk of carbon deposition in steam reforming is based on carbon number, unsaturation, and aromaticity in the feed. Carbon resistance can be enhanced by promoting catalyst with alkali. However, coking can be decreased by allowing a hydrogen-rich stream to pass through at elevated pressures [48, 139].

The mechanisms of carbon deposition on metal catalysts are different from those on oxide or sulfide catalysts. There are three different kinds of carbon species that can be observed depending on the operating conditions, catalyst formulation as relates to steam reforming of hydrocarbons over Ni-based catalysts. These are encapsulated carbon (usually obtained by slow polymerization of C_xH_y

over Ni surface at temperatures less than 500°C), filamentous or whisker-like carbon (commonly obtained by diffusion of C into Ni crystals, dissociation of Ni from the support and growth of whiskers with Ni on top), and pyrolytic-type carbon (formed as a result of cracking of C_xH_y species at temperatures greater than 600°C, and deposition of carbon precursors). It has been reported that the main pathways to coke formation in ethanol steam reforming involve: (i) methane decomposition (ii) Boudouard reaction (iii) carbon (II) oxide reduction reaction [140].

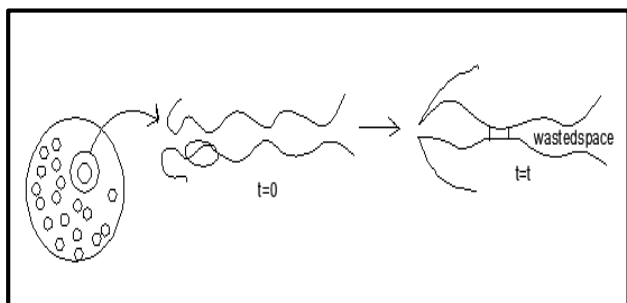


Fig. 13. Schematic diagram of catalyst decay by sintering causing pore closure [140]

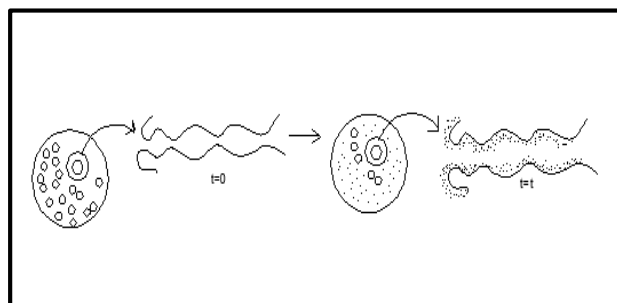


Fig. 14. Schematic diagram of catalyst decay by coking [140]

3.2 Poisoning

Catalyst poisoning is due to molecules irreversibly chemisorbed to the active sites over some time, thereby reducing active sites available for reaction. The poison molecules are generally reactants or products involved in the primary response. The two associated effects are the decrease in the catalytic sites or portion of available surface area that tends to facilitate the reaction. This increases the average distance that a reactant molecule must diffuse through the pore structure before undergoing reaction. Poisoning is similar to coking in the sense that deactivation occurs due to the deposition of constituents on the catalyst surface, but the mechanism is different. Poisoning can, by exposing the catalyst to high temperatures (1000°C). However, this also has the potential to damage the catalyst permanently [141]. Purification of reactants can prevent poisoning by impurities. The common poison for industrial processes is sulfur, as exemplified in Figure 15. At various operating conditions, hydrogen sulphide is formed from associated sulphur compounds and attaches to the active metals surfaces. This can be prevented by reacting feed gas with zinc oxide. Among the common poisons is carbon as an inhibitor of silica-alumina catalyst for cracking of petroleum; sulphur, arsenic, or lead as inhibitors of metal catalysts for hydrogenation or dehydrogenation reactions. And oxygenated water as inhibitors of iron catalysts for ammonia synthesis [142].

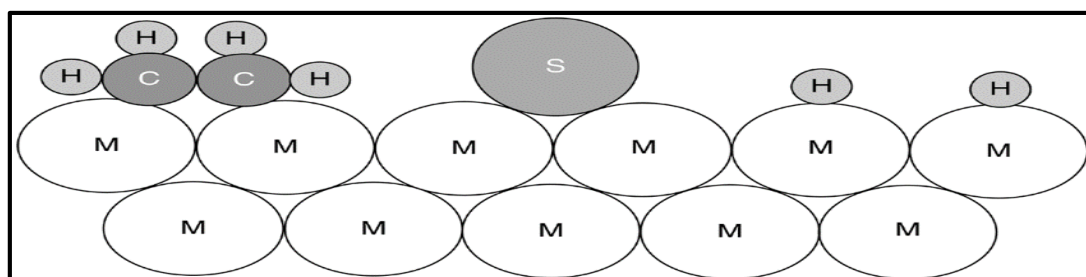


Fig. 15. Diagram of sulphur atoms poison on the metal surface for ethylene hydrogenation [142]

3.3 Catalyst Deactivation Kinetics

Catalyst ineffectiveness contributes to complications in the determination of reaction rate law parameters and pathways. In analysing reactions over decaying catalysts, kinetics is classified into separable kinetics and non-separable kinetics.

Inseparable kinetics, the rate law, and catalyst activity are dissociated. Having separable kinetics activity will create an easy independent study of catalyst decay and reaction kinetics. Whereas, in non-separable kinetics, catalyst decay and reaction kinetics are studied together [87].

$$\text{Separable kinetics: } -r_A = a(\text{history}) \times -r_A(\text{fresh catalyst}) \quad (23)$$

$$\text{Non-separable kinetics: } -r_A = -r_A(\text{history, fresh catalyst}) \quad (24)$$

With known catalyst decay, activity decreases with time, and a typical profile of activity versus time is as depicted in Figure 16.

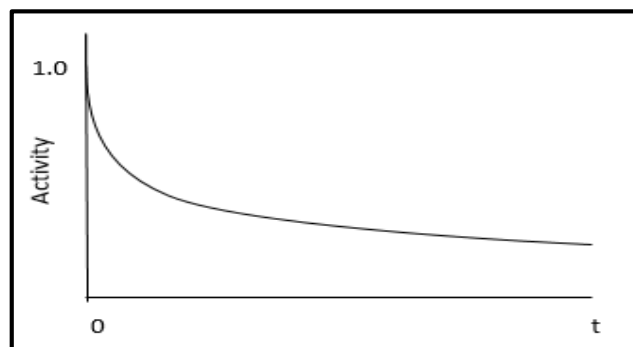


Fig. 16. Catalyst activity versus time

3.3.1 Catalyst decay kinetics by poisoning

Assuming that the rate of removal of the poison, $r_{p.s}$, from the reactant gas stream on the catalyst sites is proportional to the number of unpoisoned sites ($C_{i0} - C_{p.s}$) and the concentration of poison in the gas, C_p :

$$r_{p.s} = k_d (C_{i0} - C_{p.s}) C_p \quad (25)$$

Where $C_{p.s}$ the concentration of is poisoned sites and C_{i0} is known as the total number of available places. With the assumption that every molecule that is adsorbed from the gas phase onto a site poisoned it, this rate is also equal to the rate of removal of total active sites (C_t) from the surface.

$$\frac{dC_t}{dt} = \frac{dC_{p.s}}{dt} = r_{p.s} = k_d (C_{i0} - C_{p.s}) C_p \quad (26)$$

To express the function in terms of the fraction of the total number of sites, that have been poisoned, f , Eq. (26) is divided through by C_{i0} to yield

$$\frac{df}{dt} = k_d(1-f) C_p \quad (27)$$

The fraction of sites available for adsorption (1-f) is essentially the activity a(t). Consequently, Eq. (27) becomes [143].

$$\frac{da}{dt} = a(t) k_d C_p \quad (28)$$

3.3.2 Catalyst decay kinetics by fouling

The amount of coke on the surface after a time t has been found to obey the following empirical relationship [144]:

$$C_c = At^n \quad (29)$$

Where C_c is the concentration percentage of carbon on the surface (g/cm^3), and A and n are fouling parameters, which can be functions of feed rate. One of the commonly used tasks between the catalyst activity and the amount of coke on the surface is

$$a = \frac{1}{K_{ck} C_c^{p+1}} \quad (30)$$

when expressed in terms of time, it becomes

$$a = \frac{1}{K_{ck} A p t^{np+1}} = \frac{1}{1 + K^n t^m} \quad (31)$$

3.3.3 Catalyst decay kinetics by sintering

Deactivation by sintering, in some cases, is a function of the mainstream gas concentration. Despite several forms of sintering decay rate laws that exist, the commonly used law in second-order concerning activity:

$$r_d = K_d a^2 = -\frac{da}{dt} \quad (32)$$

With the integration, where a=1 at time t=0, yields

$$a(t) = \frac{1}{K_d t} \quad (33)$$

The amount of sintering is usually quantified as a function of the active surface area of the catalyst S_a :

$$S_a = \frac{S_{a0}}{1 + K_d t} \quad (34)$$

The sintering decay constant, K_d , follows the Arrhenius equation

$$K_d = K_d(T_o) \exp\left[\frac{E_d}{R} \left(\frac{1}{T_o} - \frac{1}{T}\right)\right] \quad (35)$$

These descriptions take into account the mechanisms of steam reforming reactions and catalyst deactivation effect on the responses. The knowledge of catalyst decay is essential because deactivation is an engineering problem that has technological and economic implications

4. Conclusion

During the catalytic conversion of oxygenated hydrocarbons, progressive deactivation of solid catalysts has economic consequences on the quantity and quality of the desired product due to resultant weak catalytic activity and selectivity of the enzyme. Because of this setback, it becomes necessary to study the reaction pathways that course activity lost and poor selectivity, including preventive measures that guaranteed cheaper, cleaner, and sustainable processes. The prominent three mechanisms of catalyst deactivation are poison, fouling, and sintering, and are mostly observed during hydrocarbons steam reforming reactions and water-gas shift reactions. However, the susceptibility of the catalyst to decay depends on its physical and chemical nature, response operating conditions, and feed purity.

In this review article, the adoption of promoters and reducible oxides supported on various active metals that have been used by multiple catalysis researchers. This is to enhance the thermal stability, mechanical resistance, catalytic performance, and catalyst selectivity have been highlighted. It is based on the review that carbon formation from steam reforming of hydrocarbon can be subdued with better interaction of active metal and support with high oxygen storage capacity during catalyst synthesis. The energetic metal particles with a smaller size, application of modifier (i.e., MgO, and CeO₂) temperature control of the catalyst bed, consideration of higher steam/ethanol molar ratio, low reduction temperature of the catalyst and optimize operating condition. Steam reforming reaction pathway of hydrocarbons is strongly dependent on the nature of catalyst and heat. A better understanding of reaction mechanisms based on the catalyst is the leading way out for sustainable and efficient energy evolution through steam reforming of oxygenated hydrocarbons like methanol, ethanol, glycerol.

Recommendations

For the sustainable production of hydrogen via steam reforming of ethanol, there is a need for the development of stable and high-performance catalysts. In this regard, the following recommendations are given by the authors:

- i. Supported-catalysts should be made of refractory and basic oxides, because of their high melting point and oxygen storage capacity, which favour stable catalyst surfaces at high temperatures.
- ii. There should be strong interaction and confinement of small crystalline size of nickel particles in the mesoporous channels of the support, to reduce carbon formation.
- iii. The limitation of Ni loading on highly necessary support should be adhered to, to avoid poor dispersion, as catalyst activity decreases per unit metal surfaces area with increasing the Ni loading above 20wt%.
- iv. The crystalline structure of the supported-catalyst should be made of sheets in strata, to stabilize the Ni metal particles and prevent them from agglomeration during the reduction and reaction stages.
- v. The thermodynamic analysis of ethanol steam reforming should be studied based on the selected Ni-based catalyst, to find out the suitable conditions at which the crystallite size of Ni is stable and free of carbon deposition.

Acknowledgement

The financial support received from the Tertiary Education Trust Fund (TETFUND) is highly acknowledged.

References

- [1] Çabuk, Saye Nihan, Alper Atak, Recep Bakış, and Alper Çabuk. "Determination of Suitable Sites for Solar Power Plants by Using Weighted Overlay Analysis: Sivrihisar Case." *International Journal of Renewable Energy Research (IJRER)* 9, no. 3 (2019): 1203-1213.
- [2] Udoye, N. E., I. P. Okokpujie, J. O. Okeniyi, J. O. Dirisu, and I. Ikpotokin. "Techno-Economic Evaluation of Coal-fired Power Plant in South-East Nigeria, a Review." *International Journal of Mechanical Engineering and Technology* 10, no. 3, (2019).
- [3] Ebshish, Ali, Zahira Yaakob, Yun Hin Taufiq-Yap, and Ahmed Bshish. "Investigation of the process conditions for hydrogen production by steam reforming of glycerol over Ni/Al₂O₃ catalyst using response surface methodology (RSM)." *Materials* 7, no. 3 (2014): 2257-2272.
<https://doi.org/10.3390/ma7032257>
- [4] Okokpujie, Imhade P., O. S. I. Fayomi, and R. O. Leramo. "The role of research in economic development." In *IOP Conference Series: Materials Science and Engineering*, vol. 413, no. 1, p. 012060. IOP Publishing, 2018.
<https://doi.org/10.1088/1757-899X/413/1/012060>
- [5] Sadooghi, Parham, and Reinhard Rauch. "Experimental and modeling study of catalytic steam reforming of methane mixture with propylene in a packed bed reactor." *International Journal of Heat and Mass Transfer* 78 (2014): 515-521.
<https://doi.org/10.1016/j.jheatmasstransfer.2014.06.084>
- [6] Eterigho, Elizabeth J., Michael A. Musa, Silver E. Ejegigbe, and I. P. Okokpujie. "Optimization of Process Parameters Influencing Biogas Production from Rumen and municipal waste: Analytical Approach." *COVENANT JOURNAL OF ENGINEERING TECHNOLOGY* 3, no. 2 (2019): 31-41.
- [7] Yahya, N. F. A., Negar Dasineh Khiavi, and N. Ibrahim. "Green electricity production by *Epipremnum aureum* and bacteria in plant microbial fuel cell." *Journal of Advanced Research in Applied Sciences and Engineering Technology* 5, no. 1 (2016): 22-31.
- [8] Chen, Junjie, and Deguang Xu. "Hydrogen Production by the Steam Reforming of Bio-Ethanol over Nickel-Based Catalysts for Fuel Cell Applications." *International Journal of Sustainable and Green Energy* 6, no. 3 (2017): 28.
<https://doi.org/10.11648/j.ijrse.20170603.11>
- [9] Okokpujie, Imhade P., Kennedy O. Okokpujie, Obinna N. Nwoke, and Joseph Azeta. "Development of a 0.5 KW horizontal Axis wind turbine." *Journal of Engineering and Applied Sciences* 13, no. 8 (2018): 2202-2208.
- [10] Odia, Osadolor O., Sunday A. Ososomi, and Princess I. Okokpujie. "Practical analysis of A small wind turbine for domestic use on latitude 7.0670 N, longitude 6.2670 E." *Journal of Research in Mechanical Engineering* 2, no. 11 (2016): 8-10.
- [11] El Murr, Doris Homsy. "Steam Reforming of Methane and Ethanol Over Co_xMg_{6-x}Al₂, Ru/Co_xMg_{6-x}Al₂ AND Cu/Co_xMg_{6-x}Al₂ Catalysts." PhD diss., University of Balamand, Faculty of Sciences, 2012.
- [12] Jin, Min-Ho, Duckkyu Oh, Ju-Hyoung Park, Chun-Boo Lee, Sung-Wook Lee, Jong-Soo Park, Kwan-Young Lee, and Dong-Wook Lee. "Mesoporous silica-supported Pd-MnO_x catalysts with excellent catalytic activity in room-temperature formic acid decomposition." *Scientific Reports* 6 (2016): 33502.
<https://doi.org/10.1038/srep33502>
- [13] Singh, Anoop, Surajbhan Sevda, Ibrahim M. Abu Reesh, Karolien Vanbroekhoven, Dheeraj Rathore, and Deepak Pant. "Biohydrogen production from lignocellulosic biomass: technology and sustainability." *Energies* 8, no. 11 (2015): 13062-13080.
<https://doi.org/10.3390/en8112357>
- [14] Manfro, Robinson L., Nielson FP Ribeiro, and Mariana MVM Souza. "Production of hydrogen from steam reforming of glycerol using nickel catalysts supported on Al₂O₃, CeO₂ and ZrO₂." *Catalysis for Sustainable Energy* 1 (2013): 60-70.
<https://doi.org/10.2478/cse-2013-0001>
- [15] Ulhiza, Tami Astie, Noor Illi Mohamad Puad, and Azlin Suhaida Azmi. "Review on biohydrogen production by dark fermentative bacteria using starch-containing waste as a substrate." *Journal of Advanced Research in Materials Science* 38, no. 1 (2017): 21-31.
- [16] Mousavi Ehteshami, Seyyed Mohsen, and Siew Hwa Chan. "Techno-economic study of hydrogen production via steam reforming of methanol, ethanol, and diesel." *Energy Technology & Policy* 1, no. 1 (2014): 15-22.
<https://doi.org/10.1080/23317000.2014.933087>

- [17] Wang, Ye, Shouzhong Zou, and Wen-Bin Cai. "Recent advances on electro-oxidation of ethanol on Pt-and Pd-based catalysts: From reaction mechanisms to catalytic materials." *Catalysts* 5, no. 3 (2015): 1507-1534.
<https://doi.org/10.3390/catal5031507>
- [18] Gaudillere, Cyril, Juan Jose González, Antonio Chica, and José M. Serra. "YSZ monoliths promoted with Co as catalysts for the production of H₂ by steam reforming of ethanol." *Applied Catalysis A: General* 538 (2017): 165-173.
<https://doi.org/10.1016/j.apcata.2017.03.008>
- [19] Møller, Kasper T., Torben R. Jensen, Etsuo Akiba, and Hai-wen Li. "Hydrogen-A sustainable energy carrier." *Progress in Natural Science: Materials International* 27, no. 1 (2017): 34-40.
<https://doi.org/10.1016/j.pnsc.2016.12.014>
- [20] Fayaz, Fahim, Long Giang Bach, Mahadi B. Bahari, Trinh Duy Nguyen, Khanh B. Vu, Ramesh Kanthasamy, Chantip Samart, Chinh Nguyen-Huy, and Dai-Viet N. Vo. "Stability evaluation of dry ethanol reforming on Lanthania-doped cobalt-based catalysts for hydrogen-rich syngas generation." *International Journal of Energy Research* 43, no. 1 (2019): 405-416.
<https://doi.org/10.1002/er.4274>
- [21] Mondal, Tarak, Kamal K. Pant, and Ajay K. Dalai. "Catalytic oxidative steam reforming of bio-ethanol for hydrogen production over Rh Promoted Ni/CeO₂-ZrO₂ catalyst." *International Journal of Hydrogen Energy* 40, no. 6 (2015): 2529-2544.
<https://doi.org/10.1016/j.ijhydene.2014.12.070>
- [22] de Lima, Sania M., Adriana M. da Silva, Lídia OO da Costa, Uschi M. Graham, Gary Jacobs, Burtron H. Davis, Lisiane V. Mattos, and Fábio B. Noronha. "Study of catalyst deactivation and reaction mechanism of steam reforming, partial oxidation, and oxidative steam reforming of ethanol over Co/CeO₂ catalyst." *Journal of Catalysis* 268, no. 2 (2009): 268-281.
<https://doi.org/10.1016/j.jcat.2009.09.025>
- [23] Souza, G., C. Ruoso, N. R. Marcilio, and O. W. Perez-Lopez. "SYNTHESIS, CHARACTERISATION AND CATALYTIC PERFORMANCE OF Cu-AND Co-MODIFIED Fe-Al CO-PRECIPIATED CATALYSTS FOR THE STEAM REFORMING OF ETHANOL." *GLOBAL NEST JOURNAL* 16, no. 6 (2014): 1111-1120.
<https://doi.org/10.30955/gnj.001483>
- [24] Souza, G., C. Ruoso, N. R. Marcilio, and O. W. Perez-Lopez. "Synthesis, Characterisation and Catalytic Performance of Cu- and Co-Modified Fe-Al Co-Precipitated Catalysts for the Steam Reforming of Ethanol." *Global Nest Journal* 16, no. 6 (2014): 1111-1120.
<https://doi.org/10.30955/gnj.001483>
- [25] Liang, Xuelian, Xinping Shi, Fanfan Zhang, Yuyang Li, Hongbin Zhang, and Youzhu Yuan. "Improved H₂ Production by Ethanol Steam Reforming over Sc₂O₃-Doped Co-ZnO Catalysts." *Catalysts* 7, no. 8 (2017): 241.
<https://doi.org/10.3390/catal7080241>
- [26] Dan, Monica, Maria Mihet, Mihaela Diana Lazar, and LIANA MURESAN. "PROMOTED ALUMINA SUPPORTED NI CATALYST FOR ETHANOL STEAM REFORMING." *Studia Universitatis Babeş-Bolyai, Chimia* 61, no. 2 (2016).
- [27] Goula, Maria A., Nikolaos D. Charisiou, Kiriakos N. Papageridis, Andreas Delimitis, Eleni Pachatouridou, and Eleni F. Iliopoulou. "Nickel on alumina catalysts for the production of hydrogen rich mixtures via the biogas dry reforming reaction: Influence of the synthesis method." *international journal of hydrogen energy* 40, no. 30 (2015): 9183-9200.
<https://doi.org/10.1016/j.ijhydene.2015.05.129>
- [28] Konsolakis, Michalis, Zisis Ioakimidis, Tzoulia Kraia, and George E. Marnellos. "Hydrogen production by ethanol steam reforming (ESR) over CeO₂ supported transition metal (Fe, Co, Ni, Cu) catalysts: Insight into the structure-activity relationship." *Catalysts* 6, no. 3 (2016): 39.
<https://doi.org/10.3390/catal6030039>
- [29] Sjöberg, Erik, Simon Barnes, Danil Korelskiy, and Jonas Hedlund. "MFI membranes for separation of carbon dioxide from synthesis gas at high pressures." *Journal of Membrane Science* 486 (2015): 132-137.
<https://doi.org/10.1016/j.memsci.2015.03.041>
- [30] Li, Gang, Masakoto Kanezashi, and Toshinori Tsuru. "Catalytic ammonia decomposition over high-performance Ru/graphene nanocomposites for efficient CO_x-free hydrogen production." *Catalysts* 7, no. 1 (2017): 23.
<https://doi.org/10.3390/catal7010023>
- [31] Chaubey, Rashmi, Satanand Sahu, Olusola O. James, and Sudip Maity. "A review on development of industrial processes and emerging techniques for production of hydrogen from renewable and sustainable sources." *Renewable and Sustainable Energy Reviews* 23 (2013): 443-462.
<https://doi.org/10.1016/j.rser.2013.02.019>

- [32] Rosen, Marc A. "The prospects for renewable energy through hydrogen energy systems." *Journal of Power and Energy Engineering* 3, no. 04 (2015): 373.
<https://doi.org/10.4236/jpee.2015.34050>
- [33] Busca, Guido, Umberto Costantino, Tania Montanari, Gianguido Ramis, Carlo Resini, and Michele Sisani. "Nickel versus cobalt catalysts for hydrogen production by ethanol steam reforming: Ni–Co–Zn–Al catalysts from hydrotalcite-like precursors." *International journal of hydrogen energy* 35, no. 11 (2010): 5356-5366.
<https://doi.org/10.1016/j.ijhydene.2010.02.124>
- [34] Saeki, Takanori, Hironobu Orkita, Noriyoshi Kakuta, and Takanori Mizushima. "Effects of Metal Oxide Support and Non-noble Metal Active Species on Catalytic Steam Reforming of Ethanol for Hydrogen Production." *Journal of the Japan Petroleum Institute* 58, no. 5 (2015): 341-350.
<https://doi.org/10.1627/jpi.58.341>
- [35] Kolb, Gunther. *Fuel processing: for fuel cells*. John Wiley & Sons, 2008.
- [36] Liguras, Dimitris K., Dimitris I. Kondarides, and Xenophon E. Verykios. "Production of hydrogen for fuel cells by steam reforming of ethanol over supported noble metal catalysts." *Applied Catalysis B: Environmental* 43, no. 4 (2003): 345-354.
[https://doi.org/10.1016/S0926-3373\(02\)00327-2](https://doi.org/10.1016/S0926-3373(02)00327-2)
- [37] Han, Seung Ju, Ji Hwan Song, Yongju Bang, Jaekyeong Yoo, Seungwon Park, Ki Hyuk Kang, and In Kyu Song. "Hydrogen production by steam reforming of ethanol over mesoporous Cu–Ni–Al₂O₃–ZrO₂ xerogel catalysts." *International Journal of Hydrogen Energy* 41, no. 4 (2016): 2554-2563.
<https://doi.org/10.1016/j.ijhydene.2015.11.128>
- [38] Calles, Jose Antonio, Alicia Carrero, Arturo Javier Vizcaíno, and Montaña Lindo. "Effect of Ce and Zr addition to Ni/SiO₂ catalysts for hydrogen production through ethanol steam reforming." *Catalysts* 5, no. 1 (2015): 58-76.
<https://doi.org/10.3390/catal5010058>
- [39] Marinho, André Luiz A., Raimundo C. Rabelo-Neto, Fabio B. Noronha, and Lisiane V. Mattos. "Steam reforming of ethanol over Ni-based catalysts obtained from LaNiO₃ and LaNiO₃/CeSiO₂ perovskite-type oxides for the production of hydrogen." *Applied Catalysis A: General* 520 (2016): 53-64.
<https://doi.org/10.1016/j.apcata.2016.03.032>
- [40] Klaewkla, Raweeewan, Matthias Arend, and Wolfgang F. Hoelderich. *A review of mass transfer controlling the reaction rate in heterogeneous catalytic systems*. Vol. 5. Rijeka: INTECH Open Access Publisher, 2011.
<https://doi.org/10.5772/22962>
- [41] Gascon, J., J. R. Van Ommen, J. A. Moulijn, and F. Kapteijn. "Structuring catalyst and reactor—an inviting avenue to process intensification." *Catalysis Science & Technology* 5, no. 2 (2015): 807-817.
<https://doi.org/10.1039/C4CY01406E>
- [42] Nabgan, Walid, Tuan Amran Tuan Abdullah, Ramli Mat, Bahador Nabgan, Yahya Gambo, and Sugeng Triwahyono. "Influence of Ni to Co ratio supported on ZrO₂ catalysts in phenol steam reforming for hydrogen production." *International Journal of Hydrogen Energy* 41, no. 48 (2016): 22922-22931.
<https://doi.org/10.1016/j.ijhydene.2016.10.055>
- [43] Cifuentes, Bernay, María Hernández, Sonia Monsalve, and Martha Cobo. "Hydrogen production by steam reforming of ethanol on a RhPt/CeO₂/SiO₂ catalyst: Synergistic effect of the Si: Ce ratio on the catalyst performance." *Applied Catalysis A: General* 523 (2016): 283-293.
<https://doi.org/10.1016/j.apcata.2016.06.014>
- [44] De, Sudipta, Jianguang Zhang, Rafael Luque, and Ning Yan. "Ni-based bimetallic heterogeneous catalysts for energy and environmental applications." *Energy & environmental science* 9, no. 11 (2016): 3314-3347.
<https://doi.org/10.1039/C6EE02002J>
- [45] Castaldo, Filomena, Vincenzo Palma, Concetta Ruocco, Paolo Ciambelli, and Gaetano Iaquaniello. "Low temperature-ethanol steam reforming over Ni-based catalysts supported on CeO₂." *Journal of Power Technologies* 95, no. 1 (2015): 54-66.
- [46] Fidalgo, Beatriz, L. Zubizarreta, José Miguel Bermúdez, A. Arenillas, and J. A. Menéndez. "Synthesis of carbon-supported nickel catalysts for the dry reforming of CH₄." *Fuel Processing Technology* 91, no. 7 (2010): 765-769.
<https://doi.org/10.1016/j.fuproc.2010.02.011>
- [47] Thyssen, Vivian V., Thaisa A. Maia, and Elisabete M. Assaf. "Cu and Ni catalysts supported on γ -Al₂O₃ and SiO₂ assessed in glycerol steam reforming reaction." *Journal of the Brazilian Chemical Society* 26, no. 1 (2015): 22-31.
<https://doi.org/10.5935/0103-5053.20140209>
- [48] Job, Nathalie, Benoît Heinrichs, Angélique Léonard, Jean-François Colomer, José Marien, and Jean-Paul Pirard. "Avoiding mass transfer limitations in carbon supported catalysis by using carbon xerogel as supports." *Chemistry for Sustainable Development* 14 (2006): 571-575.

- [49] Hassan, Faiza. "Heterogeneous catalysis in supercritical fluids: the enhancement of catalytic stability to coking." PhD diss., University of Birmingham, 2011.
- [50] Cifuentes, Bernay, Manuel Figueredo, and Martha Cobo. "Response surface methodology and aspen plus integration for the simulation of the catalytic steam reforming of ethanol." *Catalysts* 7, no. 1 (2017): 15.
<https://doi.org/10.3390/catal7010015>
- [51] Yeo, Boon Siang, and Alexis T. Bell. "Enhanced activity of gold-supported cobalt oxide for the electrochemical evolution of oxygen." *Journal of the American Chemical Society* 133, no. 14 (2011): 5587-5593.
<https://doi.org/10.1021/ja200559j>
- [52] Abad-Elwahad, Somia M., Ali F. Bukhzam, and G. A. Mekhemer. "Surface Characterization and Catalytic Activity for Alumina-Supported Cobalt Acetate." *American Journal of Materials Science* 5, no. 2A (2015): 6-9.
- [53] Eterigho, Elizabeth J., T. S. Farrow, and S. E. Ejeigbe. "Sulphated Zirconia Catalyst Prepared from Solid Sulphates by Non-aqueous Method." *IRANIAN JOURNAL OF ENERGY AND ENVIRONMENT* 8, no. 2 (2017): 142-146.
- [54] Hamzah, Noraini, and Mohd Ambar Yarmo. "Effect of Support Materials on Catalytic Activity of Nano Ruthenium Catalyst in Hydrogenolysis of Glycerol." *Malaysian Journal of Analytical Sciences* 20, no. 2 (2016): 393-400.
<https://doi.org/10.17576/mjas-2016-2002-24>
- [55] Ali, Arshid M., Muhammad A. Daous, Ahmed Arafat, Abdurraheem A. AlZahrani, Yahia Alhamed, Abudula Tuerdimaimaiti, and Lachezar A. Petrov. "Effect of Au precursor and support on the catalytic activity of the nano-Au-catalysts for propane complete oxidation." *Journal of Nanomaterials* 2015 (2015).
<https://doi.org/10.1155/2015/901439>
- [56] Zhang, Jianghao, Yaobin Li, Yan Zhang, Min Chen, Lian Wang, Changbin Zhang, and Hong He. "Effect of support on the activity of Ag-based catalysts for formaldehyde oxidation." *Scientific reports* 5 (2015): 12950.
<https://doi.org/10.1038/srep12950>
- [57] Ogo, Shuhei, Shun Maeda, and Yasushi Sekine. "Coke Resistance of Sr-Hydroxyapatite Supported Co Catalyst for Ethanol Steam Reforming." *Chemistry Letters* 46, no. 5 (2017): 729-732.
<https://doi.org/10.1246/cl.170072>
- [58] Olivares, Alejandra C. Villagrán, Manuel F. Gomez, Mariana N. Barroso, and María C. Abello. "Ni-supported catalysts for ethanol steam reforming: effect of the solvent and metallic precursor in catalyst preparation." *International Journal of Industrial Chemistry* 9, no. 1 (2018): 61-73.
<https://doi.org/10.1007/s40090-018-0135-6>
- [59] Vizcaino, A. J., A. Carrero, and J. A. Calles. "Hydrogen production by ethanol steam reforming over Cu-Ni supported catalysts." *International Journal of Hydrogen Energy* 32, no. 10-11 (2007): 1450-1461.
<https://doi.org/10.1016/j.ijhydene.2006.10.024>
- [60] Abbasi, Ali, Mohamadreza Ghasemi, and Sepehr Sadighi. "Effect of Lanthanum as a Promoter on Fe-Co/SiO₂ Catalyst for Fischer-Tropsch Synthesis." *Bulletin of Chemical Reaction Engineering & Catalysis* 9, no. 1 (2014): 23.
<https://doi.org/10.9767/bcrec.9.1.5142.23-27>
- [61] Zamani, Yahya, Akbar Zamaniyan, Farzad Bahadoran, and Mehرداد Shojaei. "Effect of Calcium Promoters on Nanostructured Iron Catalyst for Fischer-Tropsch Synthesis." *Journal of Petroleum Science and Technology* 5, no. 1 (2015): 21-27.
- [62] Dan, Monica, Maria Mihet, Mihaela Diana Lazar, and LIANA MURESAN. "PROMOTED ALUMINA SUPPORTED NI CATALYST FOR ETHANOL STEAM REFORMING." *Studia Universitatis Babeş-Bolyai, Chimia* 61, no. 2 (2016).
- [63] De Souza, G., V. C. Ávila, N. R. Marçílio, and O. W. Perez-Lopez. "Synthesis gas production by steam reforming of ethanol over M-Ni-Al hydrotalcite-type catalysts; M= Mg, Zn, Mo, Co." *Procedia Engineering* 42 (2012): 1805-1815.
<https://doi.org/10.1016/j.proeng.2012.07.575>
- [64] Lee, Youngmin, Aviva Loew, and Shouheng Sun. "Surface-and structure-dependent catalytic activity of Au nanoparticles for oxygen reduction reaction." *Chemistry of Materials* 22, no. 3 (2010): 755-761.
<https://doi.org/10.1021/cm9013046>
- [65] Dey, Subhashish, Ganesh Chandra Dhal, Devendra Mohan, and Ram Prasad. "The choice of precursors in the synthesizing of CuMnOx catalysts for maximizing CO oxidation." *International Journal of Industrial Chemistry* 9, no. 3 (2018): 199-214.
<https://doi.org/10.1007/s40090-018-0150-7>
- [66] Aiube, Carlos M., Karolyne V. de Oliveira, and Julio L. de Macedo. "Effect of Cerium Precursor in the Synthesis of Ce-MCM-41 and in the Efficiency for Liquid-Phase Oxidation of Benzyl Alcohol." *Catalysts* 9, no. 4 (2019): 377.
<https://doi.org/10.3390/catal9040377>
- [67] Jedrzejewski, Roman, and Zofia Lendzion-Bielun. "Reduction Process of Iron Catalyst Precursors for Ammonia Synthesis Doped with Lithium Oxide." *Catalysts* 8, no. 11 (2018): 494.
<https://doi.org/10.3390/catal8110494>

- [68] Zhang, Xiaodong, Yang Yang, Xutian Lv, Yuxin Wang, and Lifeng Cui. "Effects of preparation method on the structure and catalytic activity of Ag–Fe₂O₃ catalysts derived from MOFs." *Catalysts* 7, no. 12 (2017): 382.
<https://doi.org/10.3390/catal7120382>
- [69] Jhung, Sung-Hwa, Jin-Ho Lee, Jong-Min Lee, Ji-Hye Lee, Do-Young Hong, Myong-Woon Kim, and Jong-San Chang. "Effect of preparation conditions on the hydrogenation activity and metal dispersion of Pt/C and Pd/C catalysts." *Bulletin of the Korean Chemical Society* 26, no. 4 (2005): 563-568.
<https://doi.org/10.5012/bkcs.2005.26.4.563>
- [70] Lian, Zhihua, Fudong Liu, and Hong He. "Effect of preparation methods on the activity of VO_x/CeO₂ catalysts for the selective catalytic reduction of NO_x with NH₃." *Catalysis Science & Technology* 5, no. 1 (2015): 389-396.
<https://doi.org/10.1039/C4CY00935E>
- [71] Guo, Fang, Shaoqing Guo, Zegang Qiu, Liangfu Zhao, and Hongwei Xiang. "Effects of impregnation methods and drying conditions on quinoline hydrodenitrogenation over Ni-W based catalysts." *Journal of the Brazilian Chemical Society* 25, no. 4 (2014): 750-758.
<https://doi.org/10.5935/0103-5053.20140035>
- [72] Dyson, Paul J., and Philip G. Jessop. "Solvent effects in catalysis: rational improvements of catalysts via manipulation of solvent interactions." *Catalysis Science & Technology* 6, no. 10 (2016): 3302-3316.
<https://doi.org/10.1039/C5CY02197A>
- [73] Wang, Feifei, Guifen Hao, Yuming Guo, Xiaoming Ma, and Lin Yang. "Solvent Effects on Preparation of Pd-Based Catalysts: Influence on Properties of Palladium and Its Catalytic Activity for Benzyl Alcohol Oxidation." *Open Journal of Metal* 7, no. 04 (2017): 59.
<https://doi.org/10.4236/ojmetal.2017.74005>
- [74] Zou, Yongjin, Yubo Gao, Pengru Huang, Cuili Xiang, Hailiang Chu, Shujun Qiu, Erhu Yan, Fen Xu, and Lixian Sun. "Effects of the preparation solvent on the catalytic properties of cobalt–boron alloy for the hydrolysis of alkaline sodium borohydride." *Metals* 7, no. 9 (2017): 365.
<https://doi.org/10.3390/met7090365>
- [75] Pei, Yan, Gongbing Zhou, Nguyen Luan, Baoning Zong, Minghua Qiao, and Franklin Feng Tao. "Synthesis and catalysis of chemically reduced metal–metalloid amorphous alloys." *Chemical Society Reviews* 41, no. 24 (2012): 8140-8162.
<https://doi.org/10.1039/c2cs35182j>
- [76] Nayebzadeh, Hamed, Nasser Saghatoleslami, A. Maskooki, and B. Rahmani Vahid. "Effect of calcination temperature on catalytic activity of synthesis SrO/S-ZrO₂ by solvent-free method in esterification of oleic acid." *Chemical and biochemical engineering quarterly* 27, no. 3 (2013): 267-273.
- [77] Amadine, Othmane, Younes Essamlali, Aziz Fihri, Mohamed Larzek, and Mohamed Zahouily. "Effect of calcination temperature on the structure and catalytic performance of copper–ceria mixed oxide catalysts in phenol hydroxylation." *RSC advances* 7, no. 21 (2017): 12586-12597.
<https://doi.org/10.1039/C7RA00734E>
- [78] Sistani, Aliakbar, Naser Saghatoleslami, and Hamed Nayebzadeh. "Influence of calcination temperature on the activity of mesoporous CaO/TiO₂–ZrO₂ catalyst in the esterification reaction." *Journal of Nanostructure in Chemistry* 8, no. 3 (2018): 321-331.
<https://doi.org/10.1007/s40097-018-0276-3>
- [79] Akbarzadeh, Omid, Noor Asmawati Mohd Zabidi, Yasmin Abdul Wahab, Nor Aliya Hamizi, Zaira Zaman Chowdhury, Zulkifli Merican Aljunid Merican, Marlinda Ab Rahman, Shamima Akhter, Md Shalauddin, and Mohd Rafie Johan. "Effects of Cobalt Loading, Particle Size, and Calcination Condition on Co/CNT Catalyst Performance in Fischer–Tropsch Reactions." *Symmetry* 11, no. 1 (2019): 7.
<https://doi.org/10.3390/sym11010007>
- [80] Liu, Ye, Chonglin Song, Gang Lv, Chenyang Fan, and Xiaodong Li. "Promotional Effect of Cerium and/or Zirconium Doping on Cu/ZSM-5 Catalysts for Selective Catalytic Reduction of NO by NH₃." *Catalysts* 8, no. 8 (2018): 306.
<https://doi.org/10.3390/catal8080306>
- [81] Guo, Zhen, Yuanting Chen, Lusi Li, Xiaoming Wang, Gary L. Haller, and Yanhui Yang. "Carbon nanotube-supported Pt-based bimetallic catalysts prepared by a microwave-assisted polyol reduction method and their catalytic applications in the selective hydrogenation." *Journal of Catalysis* 276, no. 2 (2010): 314-326.
<https://doi.org/10.1016/j.jcat.2010.09.021>
- [82] Albretsen, Michael K., Baiyu Huang, Kamyar Keyvanloo, Brian F. Woodfield, Calvin H. Bartholomew, Morris D. Argyle, and William C. Hecker. "Effect of Drying Temperature on Iron Fischer-Tropsch Catalysts Prepared by Solvent Deficient Precipitation." *Journal of Nanomaterials* 2017 (2017).
<https://doi.org/10.1155/2017/7258650>

- [83] Saud, Anisah Sajidah Haji, Vidhyaa Paroo Indran, Nazira Talib, and Mohd Hasbi Ab Rahim. "Low Metal Loading Palladium Mixed-Oxides Catalyst for the Synthesis of Glycerol Carbonate." *Asian Journal of Applied Sciences (ISSN: 2321-0893)* 4, no. 01 (2016).
- [84] Hassan, H., and B. H. Hameed. "Fenton-like oxidation of acid red 1 solutions Using Heterogeneous catalyst based on ball clay." *International Journal of Environmental Science and Development* 2, no. 3 (2011): 218.
<https://doi.org/10.7763/IJESD.2011.V2.127>
- [85] Akhtar, Khalida, Naila Khalid, and Murad Ali. "Effect of pH and temperature on the catalytic properties of manganese dioxide." *Journal of The Chemical Society of Pakistan* 34, no. 2 (2012): 263-268.
- [86] Kim, Joo Yeon, and Hangil Lee. "Influence of pH Modification on Catalytic Activities of Metal-Doped IrO₂ Nanoparticles." *Scientific reports* 9, no. 1 (2019): 1-9.
<https://doi.org/10.1038/s41598-019-42358-9>
- [87] Dittmeyer, Roland, and Gerhard Emig. "Simultaneous heat and mass transfer and chemical reaction." *Handbook of Heterogeneous Catalysis: Online* (2008): 1727-1784.
<https://doi.org/10.1002/9783527610044.hetcat0094>
- [88] Ertl G., Knözinger H., Schüth F., Weitkamp J., (Eds.), Wiley-VCH, Weinheim, 2006, pp. 1727-1784, ISBN-13: 978-3-527-31241-2.
- [89] Manokaran, V., P. S. Saiprasad, and S. Srinath. "Studies on Heat and Mass Transfer Limitations in Oxidative Dehydrogenation of Ethane Over Cr₂O₃/Al₂O₃ Catalyst." *Procedia Engineering* 127 (2015): 1338-1345.
<https://doi.org/10.1016/j.proeng.2015.11.492>
- [90] Klaewkla, Raweewan, Matthias Arend, and Wolfgang F. Hoelderich. *A review of mass transfer controlling the reaction rate in heterogeneous catalytic systems*. Vol. 5. Rijeka: INTECH Open Access Publisher, 2011.
<https://doi.org/10.5772/22962>
- [91] Fogler, H. S. "External diffusion effects on heterogeneous reactions." *Elements of Chemical Reaction Engineering* (2006): 757-801.
- [92] Abbas, S. Z., V. Dupont, and T. Mahmud. "Kinetics study and modelling of steam methane reforming process over a NiO/Al₂O₃ catalyst in an adiabatic packed bed reactor." *International Journal of Hydrogen Energy* 42, no. 5 (2017): 2889-2903.
<https://doi.org/10.1016/j.ijhydene.2016.11.093>
- [93] Espinosa, Roger Brunet. "Structured catalysts and reactors for three phase catalytic reactions: manipulating activity and selectivity in nitrite hydrogenation." PhD Thesis, University of Twente, 2016.
- [94] Nguyet, Tran Thi Minh, Nguyen Cong Trang, Nguyen Quang Huan, Nguyen Xuan, Luu Tien Hung, and Masakazu Date. "Preparation of gold nanoparticles, Au/Fe₂O₃ by using a co-precipitation method and their catalytic activity." *Journal of the Korean Physical Society* 52, no. 5 (2008): 1345-1349.
<https://doi.org/10.3938/jkps.52.1345>
- [95] Eterigho, Elizabeth J., Jon GM Lee, and Adam P. Harvey. "Triglyceride cracking for biofuel production using a directly synthesised sulphated zirconia catalyst." *Bioresource technology* 102, no. 10 (2011): 6313-6316.
<https://doi.org/10.1016/j.biortech.2011.02.040>
- [96] Gholamrezaei, Sousan, Masoud Salavati-Niasari, Davood Ghanbari, and Samira Bagheri. "Hydrothermal preparation of silver telluride nanostructures and photo-catalytic investigation in degradation of toxic dyes." *Scientific reports* 6, no. 1 (2016): 1-13.
<https://doi.org/10.1038/srep20060>
- [97] Mu, Li, Junxi Wan, Zhenghua Wang, Yongqian Gao, and Yitai Qian. "Mn-doped zinc aluminate nanoparticles: hydrothermal synthesis, characterization, and photoluminescence properties." *Journal of nanoscience and nanotechnology* 6, no. 3 (2006): 863-867.
<https://doi.org/10.1166/jnn.2006.107>
- [98] Deraz, N. M. "The comparative jurisprudence of catalysts preparation methods: I. Precipitation and impregnation methods." *J Ind Environ Chem.* 2018; 2 (1): 19-21 (2018).
- [99] Houshiar, Mahboubeh, Fatemeh Zebhi, Zahra Jafari Razi, Ali Alidoust, and Zohreh Askari. "Synthesis of cobalt ferrite (CoFe₂O₄) nanoparticles using combustion, coprecipitation, and precipitation methods: A comparison study of size, structural, and magnetic properties." *Journal of Magnetism and Magnetic Materials* 371 (2014): 43-48.
<https://doi.org/10.1016/j.jmmm.2014.06.059>
- [100] Ingale, S. V., P. B. Wagh, D. Bandyopadhyay, I. K. Singh, R. Tewari, and S. C. Gupta. "Synthesis of nanosized platinum based catalyst using sol-gel process." In *IOP Conference Series: Materials Science and Engineering*, vol. 73, no. 1, p. 012076. IOP Publishing, 2015.
<https://doi.org/10.1088/1757-899X/73/1/012076>

- [101] de Farias, Robson F., Ulrich Arnold, Leandro Martinez, Ulf Schuchardt, Marcelo JDM Jannini, and Claudio Airoidi. "Synthesis, characterization and catalytic properties of sol-gel derived mixed oxides." *Journal of Physics and Chemistry of Solids* 64, no. 12 (2003): 2385-2389.
[https://doi.org/10.1016/S0022-3697\(03\)00276-2](https://doi.org/10.1016/S0022-3697(03)00276-2)
- [102] Machmudah, Siti, Sugeng Winardi, Hideki Kanda, and Motonobu Goto. "Synthesis of Ceria Zirconia Oxides using Solvothermal Treatment." In *MATEC Web of Conferences*, vol. 156, p. 05014. EDP Sciences, 2018.
<https://doi.org/10.1051/mateconf/201815605014>
- [103] Zhao, Xuzhao. "Solvothermal Synthesis and Characterization of CuInS₂, CuInSe₂ and AgInS₂ Nanoparticles from Single Source Precursors." (2015).
- [104] Petkovic, Lucia M., and Daniel M. Ginosar. "Comparison of Two Preparation Methods on Catalytic Activity and Selectivity of Ru-Mo/HZSM5 for Methane Dehydroaromatization." *Journal of Fuels* 2014 (2014).
<https://doi.org/10.1155/2014/364107>
- [105] Palma, Vincenzo, Concetta Ruocco, Eugenio Meloni, and Antonio Ricca. "Renewable hydrogen from ethanol reforming over CeO₂-SiO₂ based catalysts." *Catalysts* 7, no. 8 (2017): 226.
<https://doi.org/10.3390/catal7080226>
- [106] Wang, Fagen, Weijie Cai, Hélène Provendier, Yves Schuurman, Claude Descorme, Claude Mirodatos, and Wenjie Shen. "Hydrogen production from ethanol steam reforming over Ir/CeO₂ catalysts: enhanced stability by PrOx promotion." *International journal of hydrogen energy* 36, no. 21 (2011): 13566-13574.
<https://doi.org/10.1016/j.ijhydene.2011.07.091>
- [107] Akande, Abayomi John. "Production of hydrogen by reforming of crude ethanol." PhD diss., 2005.
- [108] Seelam, Prem Kumar, Anne-Riikka Rautio, Mika Huuhtanen, Krisztian Kordas, and Riitta L. Keiski. "Low temperature steam reforming of ethanol over advanced carbon nanotube-based catalysts." *Green Processing and Synthesis* 4, no. 5 (2015): 355-368.
<https://doi.org/10.1515/gps-2015-0014>
- [109] Mulewa, W., Muhammad Tahir, and N. A. S. Amin. "Ethanol Steam Reforming for Renewable Hydrogen Production over La-Modified TiO₂ Catalyst." *Chemical Engineering Transactions* 56 (2017): 349-354.
- [110] Palma, Vincenzo, Concetta Ruocco, Filomena Castaldo, Antonio Ricca, and Daniela Boettge. "Ethanol steam reforming over bimetallic coated ceramic foams: Effect of reactor configuration and catalytic support." *International Journal of Hydrogen Energy* 40, no. 37 (2015): 12650-12662.
<https://doi.org/10.1016/j.ijhydene.2015.07.138>
- [111] Chen, Junjie, and Deguang Xu. "Hydrogen Production by the Steam Reforming of Bio-Ethanol over Nickel-Based Catalysts for Fuel Cell Applications." *International Journal of Sustainable and Green Energy* 6, no. 3 (2017): 28.
<https://doi.org/10.11648/j.ijrse.20170603.11>
- [112] Anamika, S., and K. K. Pant. "Oxidative Steam Reforming of Bioethanol over Rh/CeO₂-Al₂O₃ Catalyst for Hydrogen Production." *J Thermodyn Catal* 4, no. 119 (2013): 2.
- [113] Su, Dong. "Advanced electron microscopy characterization of nanomaterials for catalysis." *Green Energy & Environment* 2, no. 2 (2017): 70-83.
<https://doi.org/10.1016/j.gee.2017.02.001>
- [114] Chaturvedi, Shalini, and Pragnesh N. Dave. "Electron microscopy in heterogenous catalysis." *Microscopy: Science, Technology, Applications and Education* (2014): 813-818.
- [115] Saib, A. M., D. J. Moodley, I. M. Ciobîcă, M. M. Hauman, B. H. Sigwebela, C. J. Weststrate, J. W. Niemantsverdriet, and J. Van de Loosdrecht. "Fundamental understanding of deactivation and regeneration of cobalt Fischer-Tropsch synthesis catalysts." *Catalysis Today* 154, no. 3-4 (2010): 271-282.
<https://doi.org/10.1016/j.cattod.2010.02.008>
- [116] Bunaciu, Andrei A., Elena Gabriela Udriștioiu, and Hassan Y. Aboul-Enein. "X-ray diffraction: instrumentation and applications." *Critical reviews in analytical chemistry* 45, no. 4 (2015): 289-299.
<https://doi.org/10.1080/10408347.2014.949616>
- [117] Sie, Min-Chun, Pei-Di Jeng, Pin-Hsuan Chen, Ruei-Ci Wu, and Chen-Bin Wang. "Evaluation of CO oxidation over Co₃O₄-supported NiO catalysts." In *AIP Conference Proceedings*, vol. 1877, no. 1, p. 070004. AIP Publishing LLC, 2017.
<https://doi.org/10.1063/1.4999890>
- [118] Pakhare, Devendra. "Catalytic Active Site, Mechanistic and Kinetic Studies of Dry (CO₂) Reforming of Methane over Lanthanum Zirconate (La₂Zr₂O₇) Pyrochlores." (2014).
<https://doi.org/10.1016/j.jcat.2014.04.023>
- [119] Wu, Chunfei, Valerie Dupont, Mohamad Anas Nahil, Binlin Dou, Haisheng Chen, and Paul T. Williams. "Investigation of Ni/SiO₂ catalysts prepared at different conditions for hydrogen production from ethanol steam reforming." *Journal of the Energy Institute* 90, no. 2 (2017): 276-284.

- <https://doi.org/10.1016/j.joei.2016.01.002>
- [120] Akande, Abayomi J., Raphael O. Idem, and Ajay K. Dalai. "Synthesis, characterization and performance evaluation of Ni/Al₂O₃ catalysts for reforming of crude ethanol for hydrogen production." *Applied Catalysis A: General* 287, no. 2 (2005): 159-175.
<https://doi.org/10.1016/j.apcata.2005.03.046>
- [121] Wu, Chunfei, and Paul T. Williams. "Investigation of coke formation on Ni-Mg-Al catalyst for hydrogen production from the catalytic steam pyrolysis-gasification of polypropylene." *Applied Catalysis B: Environmental* 96, no. 1-2 (2010): 198-207.
<https://doi.org/10.1016/j.apcatb.2010.02.022>
- [122] Wu, Chunfei, and Paul T. Williams. "A novel nano-Ni/SiO₂ catalyst for hydrogen production from steam reforming of ethanol." *Environmental science & technology* 44, no. 15 (2010): 5993-5998.
<https://doi.org/10.1021/es100912w>
- [123] Awad, Ali, Abdus Salam, and Bawadi Abdullah. "Thermocatalytic decomposition of methane/methanol mixture for hydrogen production: Effect of nickel loadings on alumina support." In *AIP conference proceedings*, vol. 1891, no. 1, p. 020030. AIP Publishing LLC, 2017.
<https://doi.org/10.1063/1.5005363>
- [124] Baravkar, A. A., R. N. Kale, and S. D. Sawant. "FTIR Spectroscopy: principle, technique and mathematics." *International Journal of Pharma and Bio Sciences* 2, no. 1 (2011): 513-519.
- [125] Tang, Juntao, and Jianlong Wang. "Fe-based metal organic framework/graphene oxide composite as an efficient catalyst for Fenton-like degradation of methyl orange." *RSC advances* 7, no. 80 (2017): 50829-50837.
<https://doi.org/10.1039/C7RA10145G>
- [126] YU, Yan-ke, H. E. Chi, Jin-sheng CHEN, and Xiao-ran MENG. "Deactivation mechanism of de-NO_x catalyst (V₂O₅-WO₃/TiO₂) used in coal fired power plant." *Journal of Fuel Chemistry and Technology* 40, no. 11 (2012): 1359-1365.
[https://doi.org/10.1016/S1872-5813\(13\)60003-1](https://doi.org/10.1016/S1872-5813(13)60003-1)
- [127] Sing, Kenneth. "The use of nitrogen adsorption for the characterisation of porous materials." *Colloids and Surfaces A: Physicochemical and Engineering Aspects* 187 (2001): 3-9.
[https://doi.org/10.1016/S0927-7757\(01\)00612-4](https://doi.org/10.1016/S0927-7757(01)00612-4)
- [128] Olafadehan, O. A., A. A. Ayoola, O. O. Akintunde, and V. O. Adeniyi. "Mechanistic kinetic models for steam reforming of concentrated crude ethanol on Ni/Al₂O₃ catalyst." *Journal of Engineering Science and Technology* 10, no. 5 (2015): 633-653.
- [129] Etemadi, Samaneh. "Catalytic investigations of zeolite based methanol to hydrocarbons catalysts." Master's thesis, Universitas of Oslo, 2015.
- [130] Silberova, B. Aeijelts Averink, M. Makkee, and J. A. Moulijn. "Mechanism of deactivation of Au/Fe₂O₃ catalysts under water-gas shift conditions." *Topics in Catalysis* 44, no. 1-2 (2007): 209-221.
<https://doi.org/10.1007/s11244-007-0294-8>
- [131] Resini, Carlo, Carlo Lucarelli, Melanie Taillades-Jacquin, Kan-Ern Liew, Ilenia Gabellini, Stefania Albonetti, David Wails, Jacques Roziere, Angelo Vaccari, and Deborah Jones. "Pt-Sn/γ-Al₂O₃ and Pt-Sn-Na/γ-Al₂O₃ catalysts for hydrogen production by dehydrogenation of Jet A-1 fuel: Characterisation and preliminary activity tests." *international journal of hydrogen energy* 36, no. 10 (2011): 5972-5982.
<https://doi.org/10.1016/j.ijhydene.2011.02.036>
- [132] ŞİMŞEK, VELİ, LEVENT DEĞİRMENCİ, and KIRALI MÜRTEZAOĞLU. "Sustainable activity of hydrothermally synthesized mesoporous silicates in acetic acid esterification." *Turkish Journal of Chemistry* 39, no. 3 (2015): 683-696.
<https://doi.org/10.3906/kim-1411-17>
- [133] Phil, Ha Heon, Maddigapu Pratap Reddy, Pullur Anil Kumar, Lee Kyung Ju, and Jung Soon Hyo. "SO₂ resistant antimony promoted V₂O₅/TiO₂ catalyst for NH₃-SCR of NO_x at low temperatures." *Applied Catalysis B: Environmental* 78, no. 3-4 (2008): 301-308.
<https://doi.org/10.1016/j.apcatb.2007.09.012>
- [134] Maksimowski, Paweł, Tomasz Gołofit, and Waldemar Tomaszewski. "Palladium Catalyst in the HBIW Hydrodebenzylation Reaction. Deactivation and Spent Catalyst Regeneration Procedure." *Central European Journal of Energetic Materials* 13, no. 2 (2016): 333-348.
<https://doi.org/10.22211/cejem/64988>
- [135] Leshnov, Marissa, and Matthew Yung. "Effects of metal impregnation on ZSM-5 for catalytic upgrading of biofuel intermediates." *The University of Alabama, Tuscaloosa, AL* (2015).
- [136] Mustafa, M. A., and Mert Atilhan. "Investigation on the Deactivation of Residue Fluid Catalytic Cracking (FCC) Catalyst." *International Journal of Materials Chemistry and Physics* 1, no. 2 (2015): 146-155.

- [137] AlSawalha, M., F. Roessner, L. Novikova, and L. Bel'chinskaya. "Acidity of different Jordanian Clays characterized by TPD-NH₃ and MBOH Conversion." *World Acad. Sci. Eng. Technol* 5 (2011): 7-29.
- [138] Yao, Min, Dongyue Wang, and Min Zhao. "Element analysis based on energy-dispersive X-ray fluorescence." *Advances in Materials Science and Engineering* 2015 (2015).
<https://doi.org/10.1155/2015/290593>
- [139] Argyle, Morris D., and Calvin H. Bartholomew. "Heterogeneous catalyst deactivation and regeneration: a review." *Catalysts* 5, no. 1 (2015): 145-269.
<https://doi.org/10.3390/catal5010145>
- [140] Sehested, Jens, Johannes AP Gelten, Ioannis N. Remediakis, Hanne Bengaard, and Jens K. Nørskov. "Sintering of nickel steam-reforming catalysts: effects of temperature and steam and hydrogen pressures." *Journal of Catalysis* 223, no. 2 (2004): 432-443.
<https://doi.org/10.1016/j.jcat.2004.01.026>
- [141] Nasrallah M, Deraz. "Sintering process and catalysis." *International Journal of Nanomaterials, Nanotechnology, and Nanomedicine* 4, no. 1 (2018).
<https://doi.org/10.17352/2455-3492.000023>
- [142] Katare, Santhoji, and Paul M. Laing. *A hybrid framework for modeling aftertreatment systems: A diesel oxidation catalyst application*. No. 2006-01-0689. SAE Technical Paper, 2006.
<https://doi.org/10.4271/2006-01-0689>
- [143] Halabi, M. H., M. H. J. M. De Croon, J. Van der Schaaf, P. D. Cobden, and J. C. Schouten. "Low temperature catalytic methane steam reforming over ceria-zirconia supported rhodium." *Applied Catalysis A: General* 389, no. 1-2 (2010): 68-79.
<https://doi.org/10.1016/j.apcata.2010.09.004>
- [144] Tayal, Prateek. "Light off temperature based approach to determine diesel oxidation catalyst effectiveness level and the corresponding outlet NO and NO₂ characteristics." Master's Thesis, Purdue University, 2014.